Technical Report Number 4

AN ANALYTICAL EVALUATION OF THE MILLS CROSS AND
THE TWO-DIMENSIONAL MATRIX ANTENNA ARRAY

Prepared By

Radio Frequency Tracking Laboratory

E. R. Graf, Technical Director

May 15, 1964

CONTRACT NAS8-5231

GEORGE C. MARSHALL SPACE FLIGHT CENTER

NATIONAL AERONAUTICS AND SPACE ADMINISTRATION

HUNTSVILLE, ALABAMA

APPROVED BY

C. H. Weaver
Head Professor
Electrical Engineering

SUBMITTED BY

H. M. Summer
Project Leader

TABLE OF CONTENTS

LIST OF FIGURES

AN ANALYTICAL EVALUATION OF THE MILLS CROSS AND THE TWO-DIMENSIONAL MATRIX ANTENNA ARRAY

L. C. Martin and E. R. Graf

I. INTRODUCTION

This study consists of an analytical evaluation of the Mills cross antenna array and the two-dimensional matrix antenna array when crossed-slot antennas are used as array elements. The investigation includes the determination of the field intensity patterns of both arrays and a comparison of the beam widths and the directivities.

The Mills cross antenna array[1] is a type of radio telescope antenna which produces a pencil beam of high resolution. The array was developed in 1953 by B. Y. Mills and A. G. Little who had observed that, although narrow beamwidths are desirable for radio astronomy antennas, the gains of the antennas are relatively unimportant. The Mills cross was developed to take advantage of these observations and thus to produce the pencil beamwidths of large conventional arrays but with relatively low gains and relatively small costs.

The Mills cross consists of two long arrays which are situated at right angles to one another in the form of a cross, as illustrated in Figure 1. The field pattern of each array is a fan beam which is broad in the plane perpendicular to the array axis and which is relatively narrow in a plane containing the array. When the responses of the two arrays are combined in the same phase, the resulting field pattern is the superposition of the patterns of each array. In the plane containing

---

[1] B. Y. Mills, A. G. Little, K. V. Sheridan, O. B. Slee, "A High Resolution Radio Telescope for use at 3.5 Meters," _Proceedings of the I.R.E._, 46:67-84, January, 1958.
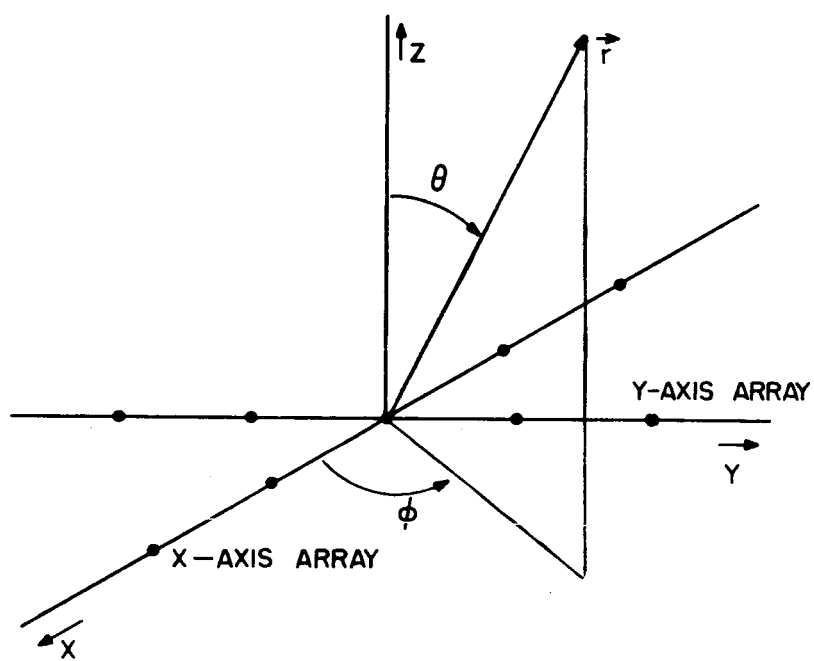
FIGURE 1   THE MILLS CROSS ARRAY CONFIGURATION

both arrays, the total pattern is a cross with the central portion enhanced by 3db. When the responses are combined in phase opposition, the total pattern in the plane of the arrays is a cross with the central portion diminished. In Figure 2, an idealized radiation pattern of the Mills cross array illustrates the interaction of the fan beam.

The pencil beam response of the Mills cross is formed by mixing the outputs of the two arrays alternately in equal and opposite phase at some given rate. Signals originating from a direction near the intersection of the two fan beams will have modulation imposed upon them which is at the switching frequency. Other signals which illuminate the array from some different direction will have no modulation imposed. Hence, if after detection, only the modulation frequency component of the combined signal is retained, the response of the system is confined to the region of the intersection of the two fan beams and an effective pencil beam results.

If the responses of the two arrays are multiplied by the principle of pattern multiplication, the combined response will be that which would be obtained from a two-dimensional matrix antenna array composed of as many rows as there are elements in one arm of the cross and as many columns as there are elements in the other arm of the cross. Figure 3 illustrates a two dimensional matrix antenna array.

A beam scanning antenna is one in which the direction of the main beam of the radiated energy may be shifted by varying one or more parameters associated with the antenna. Such antennas are becoming highly desirable in modern applications since they do not require the movement
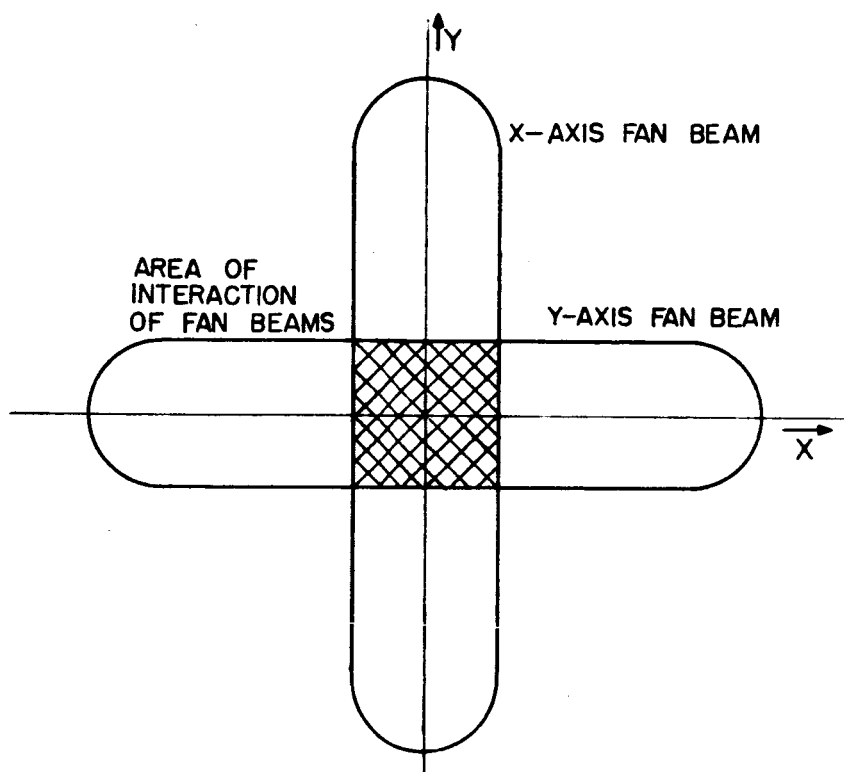
FIGURE 2 RADIATION PATTERN OF MILLS CROSS ARRAY SHOWING THE AREA OF INTERACTION OF FAN BEAMS
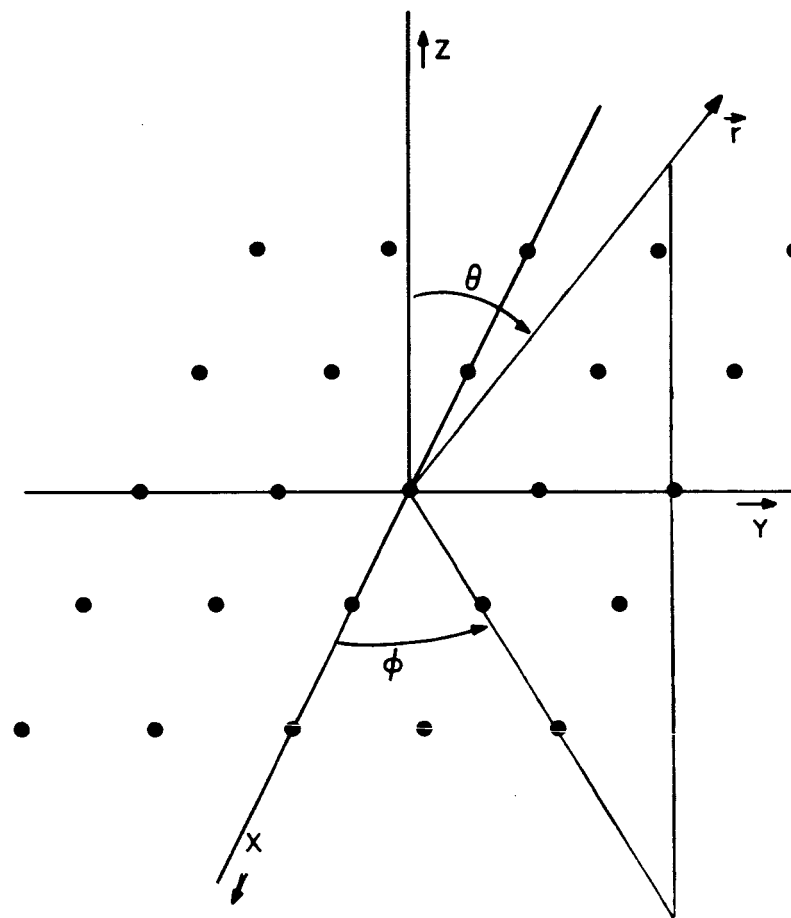
FIGURE 3 THE TWO-DIMENSIONAL MATRIX ARRAY CONFIGURATION

of large masses. Instead, a change such as the position of a primary

feed or the phase relationship between elements may scan the antenna

over the desired sector. Of particular interest is the electronically

scanned antenna in which there is no mechanical movement of hardware

on the antenna. The beam of these antennas may be shifted to any

direction almost instantaneously and may scan an entire hemisphere in

only a few seconds of time.

Ideally, an electronically scanned antenna should be capable of

pointing its main beam in any direction without deterioration of the

beam shape or the directivity. Since this is generally impossible to

accomplish, it is sufficient to say that it is desirable to shift the

beam over a defined sector with little deterioration in beam shape or

directivity and with the side lobe level continuously below some pre-

scribed level.

The maximum volume of the scanned sector of an electronically

scanned antenna is determined by the radiation pattern of the individual

array elements, by the spacing between elements, and by the mutual

coupling between elements.[2] Thus if the beam is to be scanned through-

out a hemisphere, each element of the antenna array must possess a

component of electric field throughout the hemisphere.

The Mills cross antenna array and the two-dimensional matrix antenna

array are capable of being scanned electronically by simply changing the

differential phase shift between array elements.

[2] Harold Shnitkin, "A Survey of Electronically Scanned Antennas - Part I," <u>Microwave Journal</u>, 3:68, October, 1960.

It is the purpose of this study to show the beam shape deteriorations and the change in directivity as the beam is scanned throughout a hemisphere. An antenna element is chosen to provide the capability of hemispherical scanning. Also a criterion is discussed which will reduce or control the side lobe level.

II. ANALYTICAL DEVELOPMENT

The Crossed-Slot Antenna as an Array Element

The crossed-slot antenna exhibits several characteristics which
make it desirable for use in a scanned beam array. The element is
nearly symmetrical, it has no nulls in the electric field, and it
may be circularly polarized in the axial direction. The crossed-slot
antenna is composed of two mutually perpendicular, narrow slots in a
thin, infinite ground plane. The slots may be backed by a cavity to
eliminate the radiation from one side of the ground plane and thus to
increase the efficiency of the radiators.

The duality principle, as postulated by H. G. Booker[3], states that
the radiation pattern of a slot in an infinite ground plane is the same
as that of the complementary dipole antenna except that the electric
and magnetic fields are interchanged and that the component of electric
field of the slot normal to the sheet is discontinuous from one side of
the sheet to the other.

Consider two, one-half wavelength electric dipoles. Let one dipole
be placed on the x-axis and the other on the y-axis with each of the
centers at the origin of the coordinate system indicated in Figure 1.
In the far field, the normalized components of the magnetic field

[3]John D. Kraus, Antennas (New York: McGraw-Hill Book Company, 1950),
pp. 356-357, citing H. G. Booker, "Slot Aerials and Their Relation to
Complementary Wire Aerials," J.I.E.E. (London), 93, Part IIA, No. 4
1946.

intensity of the x-axis dipole and the y-axis dipole are respectively

$$H_{\Theta x} = \frac{\sin \phi \, \cos \, (\pi/2 \, \sin \Theta \, \cos \phi)}{1 - \sin^2 \Theta \, \cos^2 \phi} \tag{1}$$

$$H_{\phi x} = \frac{\cos \Theta \, \cos \phi \, \cos \, (\pi/2 \, \sin \Theta \, \cos \phi)}{1 - \sin^2 \Theta \, \cos^2 \phi} \quad, \tag{2}$$

and

$$H_{\Theta y} = \frac{\cos \phi \cdot \cos \, (\pi/2 \, \sin \Theta \, \sin \phi)}{1 - \sin^2 \Theta \, \sin^2 \phi} \tag{3}$$

$$H_{\phi y} = \frac{\cos \Theta \, \sin \phi \, \cos \, (\pi/2 \, \sin \Theta \, \sin \phi)}{1 - \sin^2 \Theta \, \sin^2 \phi} \tag{4}$$

The equations of the normalized electric field intensities may be ob-
tained for the complementary slot antennas by applying the duality
principle to the dipole antennas whose normalized magnetic field in-
tensities are given by equations 1 through 4. Thus, a resonant slot
which is one-half wavelength long and which is centered on the x-axis
has a normalized electric field which may be expressed as

$$E_{\Theta x} = \frac{\sin \phi \cos (\pi/2 \sin \Theta \cos \phi)}{1 - \sin^2 \Theta \cos^2 \phi} \quad , \tag{5}$$

and

$$E_{\phi x} = \frac{\cos \Theta \cos \phi \cos (\pi/2 \sin \Theta \cos \phi)}{1 - \sin^2 \Theta \cos^2 \phi} \quad . \tag{6}$$

Similarly a half wavelength resonant slot which is centered on the y-axis has a normalized electric field which may be expressed as

$$E_{\Theta y} = \frac{\cos \phi \cos (\pi/2 \sin \Theta \sin \phi)}{1 - \sin^2 \Theta \sin^2 \phi} \quad , \tag{7}$$

and

$$E_{\phi y} = \frac{\cos \Theta \sin \phi \cos (\pi/2 \sin \Theta \sin \phi)}{1 - \sin^2 \Theta \sin^2 \phi} \quad . \tag{8}$$

A crossed-slot antenna composed of two perpendicular slot antennas which are fed in phase quadrature will have a normalized electric field intensity pattern which is formed by the vector addition of the electric field patterns of the two slots. The Θ-component of the combined fields of the crossed-slot element may be expressed as

$$E_{e\theta} = E_{\theta x} - j \ E_{\theta y} \quad , \tag{9}$$

where the negative (-) sign indicates that the component of field from the y-axis lags that from the x-axis to produce right-hand elliptical polarization[4]. Combining equations 5, 7, and 9, the θ-component becomes

$$E_{e\theta} = \frac{\sin \phi \ \cos \ (\pi/2 \ \sin \theta \ \cos \phi)}{1 - \sin^2 \theta \ \cos^2 \phi}$$

$$\tag{10}$$

$$\frac{- j \ \cos \phi \ \cos \ (\pi/2 \ \sin \theta \ \sin \phi)}{1 + \sin^2 \theta \ \sin^2 \phi} \quad .$$

Similarly, the ϕ-component of the combined fields of the crossed-slot element may be expressed as

$$E_{e\phi} = E_{\phi x} - j \ E_{\phi y} \quad . \tag{11}$$

Combining equations 6, 8, and 11, the ϕ-component becomes

$$E_{e\phi} = \frac{\cos \theta \ \cos \phi \ \cos \ (\pi/2 \ \sin \theta \ \cos \phi)}{1 - \sin^2 \theta \ \cos^2 \phi}$$

$$\tag{12}$$

$$\frac{- j \ \cos \theta \ \cos \phi \ \cos \ (\pi/2 \ \sin \theta \ \cos \phi)}{1 - \sin^2 \theta \ \sin^2 \phi} \quad .$$

---

[4]Ibid., pp. 464-467.

Equations 10 and 12 are the pattern factors of the components of the electric field intensity of the crossed-slot antenna which will be employed as the array element. The normalized field intensity patterns of these components show that the θ-components of the field is present through-out the hemisphere and that the magnitude of the component varies only 1db from its maximum value. Figure 4 shows a comparison of the unit circle to the normalized field pattern of the θ-component of the crossed slot in the plane of $\phi = 45^o$, where the maximum variation occurs. The ϕ-component is more directive and is nonexistent in the plane of the slots. The normalized field pattern of this component has a half-power beamwidth of approximately 80°. Figure 4 also illustrates the normalized field pattern of the ϕ-component of the crossed slot antenna in the plane $\phi = 45^o$.

The Mills Cross Array

The Mills cross antenna array is composed of two linear arrays which are crossed at right angles as illustrated in Figure 1. To obtain the equations of the response of the total array, the field equations of each arm of the cross may be obtained separately. Then the two responses may be combined in the prescribed manner. In considering the separate arms of the cross, it is a straight-forward procedure to first determine the field equations assuming the array to be composed of isotropic point source radiators and then replace each point source with the array element by the principles of pattern multiplication[6].

---

[6]Ibid., pp. 66-67.

13
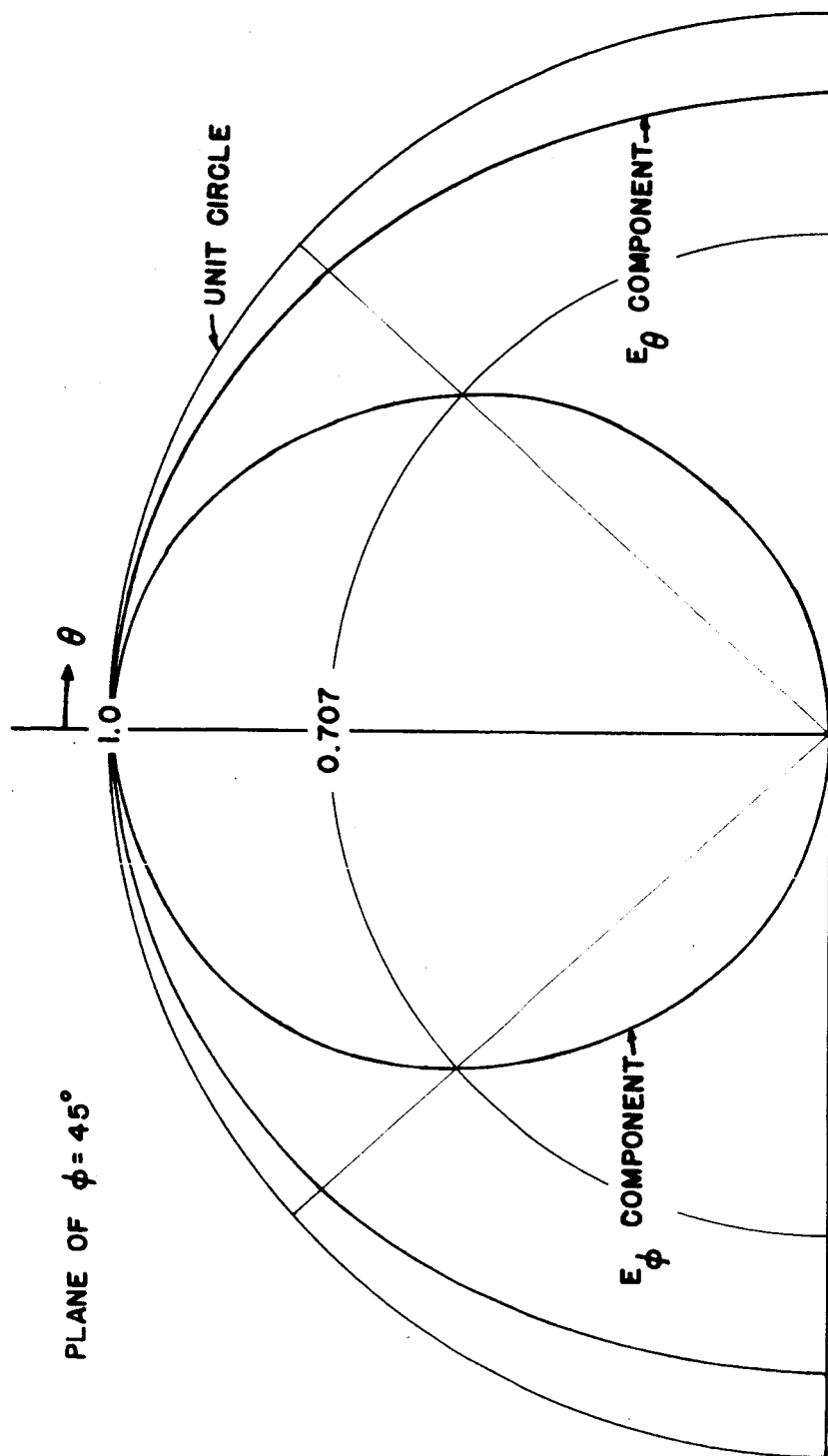
FIGURE 4   THE NORMALIZED FIELD PATTERN OF THE CROSSED SLOT ANTENNA IN THE PLANE OF THE MAXIMUM VARIATION OF THE E_θ-COMPONENT

The array on the x-axis, which is composed of N radiators fed with equal current magnitudes and whose phase reference is the center of the array, will have a relative electric field intensity pattern given by[7]

$$E_x = \frac{\sin\left(\frac{N\psi_x}{2}\right)}{N\sin\left(\frac{\psi_x}{2}\right)} \quad , \tag{13}$$

where $\psi_x = 2\pi d_\lambda \sin\theta \cos\phi + \partial_x$.

Here d_λ is the spacing between elements in wavelengths and ∂_x is the relative phase between elements. Likewise, the y-axis array will have a relative field pattern given by

$$E_y = \frac{\sin\left(\frac{N\psi_y}{2}\right)}{N\sin\left(\frac{\psi_y}{2}\right)} \quad , \tag{14}$$

where $\psi_y = 2\pi d_\lambda \sin\theta \sin\phi + \partial_y$.

By the principles of pattern multiplication, the total electric field patterns of the arrays of crossed-slot antennas on the x-axis and the y-axis are respectively

$$\overline{E}_{Ax} = E_x \left[E_{e\theta}\overline{a}_\theta + E_{e\phi}\,\overline{a}_\phi \right] \quad , \tag{15}$$

---

[7]Ibid., pp. 76-78.

and

$$\overline{E}_{Ay} = E_y \left[E_{e\theta} \ \overline{a}_\theta + E_{e\phi} \ \overline{a}_\phi \right] \quad .$$ (16)

Let V_{AX} and V_{AY} represent the complex voltages present at the mixing point of the x-axis array and the y-axis array respectively when energy is incident upon the arrays from a direction fixed by θ and ϕ[8]. The power output from the antenna system when the arrays are combined in phase addition is given by[9]

$$W_i = K_1 (V_{AX} + V_{AY})(V_{AX} + V_{AY})^* \quad .$$ (17)

Likewise, when the arrays are combined 180° out of phase, the power output is given by

$$W_o = K_1 (V_{AX} - V_{AY})(V_{AX} - V_{AY})^* \quad .$$ (18)

The total power output is

$$W_T = W_i \ f_1 \ (\omega_s t) + W_o \ f_2 \ (\omega_s t) \quad .$$ (19)

$f_1 (\omega_s t)$ and $f_2 (\omega_s t)$ are switching functions which may be represented in one period as

---

[8]Mills, et. al., op. cit., p. 69.

[9]Walter W. Lewis, and Clarence F. Goodhart, <u>Basic Electric Circuit Theory</u> (New York: The Ronald Press Company, 1958), pp. 82-84.

$$f_1(\omega_s t) = \begin{cases} 1 \text{ for } 0 < \omega_s t < \pi \\ 0 \text{ for } \pi < \omega_s t < 2\pi \end{cases} , \qquad (20)$$

and

$$f_2(\omega_s t) = \begin{cases} 0 \text{ for } 0 < \omega_s t < \pi \\ 1 \text{ for } \pi < \omega_s t < 2\pi \end{cases} , \qquad (21)$$

where ω_s is the fundamental angular switching rate.

From Fourier analysis[10], equation 20 and 21 may be expressed as

$$f_1(\omega_s t) = 1/2 + 2/\pi \sum_{\substack{n \\ n \text{ odd}}}^{\infty} \frac{\sin(n\omega_s t)}{n} , \qquad (22)$$

and

$$f_2(\omega_s t) = 1/2 - 2/\pi \sum_{\substack{n \\ n \text{ odd}}}^{\infty} \frac{\sin(n\omega_s t)}{n} . \qquad (23)$$

Then the total power may be written as

$$W_T = 1/2 (W_i + W_o) + (W_i - W_o) 2/\pi \sum_{\substack{n \\ n \text{ odd}}}^{\infty} \frac{\sin(n\omega_s t)}{n} . \qquad (24)$$

---

[10]Robert W. Landee, Donavan C. Davis, Albert P. Albrecht, Electronic Designers' Handbook, (New York: McGraw Hill Book Company, 1957), pp. 103-107.

Writing out several terms of equation 23, the total power is

$$W_T = 1/2 \ (W_i + W_o) + (W_i - W_o) \ 2/\pi \left[\ \sin \ (\omega_s t) \right.$$

$$\left. + \ 1/3 \ \sin \ (3 \ \omega_s t) + 1/5 \ \sin \ (5 \ \omega_s t) + \ldots \ \right] \ . \tag{25}$$

By assuming that the switching frequency, ω_s, is small compared to the carrier frequency of the radio-frequency signal, the received power may be detected with a square-law device[11] and the output taken through a low pass filter. The peak amplitude of the modulated signal is then

$$A_m = K_o \ (W_i - W_o) \ , \tag{26}$$

where K_o is a constant determined by the characteristics of the detector and the low pass filter.

Upon substituting equations 17 and 18 into equation 26 and simplifying, the peak amplitude of the recorded response of the Mills-cross array system is obtained and is given by

$$A_m = 4 \ K \left[\ V_{ax} \ V_{ay} \ \right] \ , \tag{27}$$

where $K = K_o K_1$.

---

[11]Mills, _et al._, _op. cit._, pp. 70-71.

It has been shown, therefore, that the recorded response of the Mills cross array is proportional to E_{Ax} and E_{Ay} as defined in equations 15 and 16 respectively.

The Two-Dimensional Matrix Antenna Array

The two-dimensional matrix antenna array is composed of N rows of element antennas with N elements in each row. The two-dimensional matrix array is illustrated in Figure 3 on page 5. The response of the array is obtained directly by summing the energy received by all the N^2 element antennas. The principle of pattern multiplication may be applied to obtain the field pattern equations of the array[12]. Multiplying equations 13 and 14 to obtain the pattern factor for the matrix array of isotropic point sources and then multiplying by the element factor, the total equation for the electric field intensity of the matrix array is given by

$$\overline{E}_m = E_x \, E_y \, \overline{E}_e \quad . \tag{28}$$

Equation 28 may be broken into its vector components such that

$$E_{m\theta} = E_x \, E_y \, E_{e\theta} \quad ,$$

and

$$E_{m\phi} = E_x \, E_y \, E_{e\phi} \quad . \tag{29}$$

---

[12]Kraus, op. cit., pp. 66-67.

In equation 28, the field pattern of the two dimensional matrix array has been shown to be the product of the field intensity patterns of one row and one column of the matrix of elements. Comparing these results with the results of the analysis of the Mills cross array, it may be seen that for the Mills cross array, the patterns of two linear arrays of N elements each have been combined to produce an effective pattern which is equivalent to that of a two-dimensional array consisting of N/2 times more elements[13].

Beam Scanning by Elemental Phase Variation

In the synthesis of the field equations for the array, a method suggests itself with which the beam of the array may be steered. Since the field pattern of the element antenna is assumed fixed, regardless of its position in the array, the array factor provides the only method for changing the direction of the beam maximum.

Consider the pattern factor of the linear array of N isotropic radiators given by equation 13. It is clear that E_x has its absolute maximum value when the argument of both numerator and denominator are zero. Thus $E_x(max)$ occurs when

$$2\pi d_\lambda \sin \theta \cos \phi + \partial_x = 0 \tag{30}$$

where $\bar{\theta}$ and $\bar{\phi}$ define the direction in which E_x is a maximum.

___

[13]A. Ksienski, "Signal Processing Antennas - Part I," _Microwave Journal_, 4:79, October, 1961.

If d_λ in equation 30 remains fixed for a given array, the only parameter which can change the direction of the beam maximum is the elemental phase shift, ∂_x. Likewise, in the pattern factor of the linear array given by equation 14, it is evident that the elemental phase shift, ∂_y, affects the direction of the beam in a similar manner.

When equations 13 and 14 are combined to produce the array factor, it is apparent that when either the beam direction or the elemental phase shift is specified, the other parameter is simultaneously defined by the solution of the equations

$$\partial_x = - 2\pi d_\lambda \sin \overline{\theta} \cos \overline{\phi} \quad , \tag{31}$$

and

$$\partial_y = - 2\pi d_\lambda \sin \theta \sin \phi \quad . \tag{32}$$

An Optimum Element Spacing for Reduction of Side Lobes

One of the major drawbacks in scanned arrays is the appearance of secondary lobes in the patterns as the beam is scanned from broadside. Shnitkin[14] suggests that a limitation be placed upon the element spacing, d_λ, in order to reduce the grating lobe for a desired scan volume.

Consider the pattern factor of the linear array of isotropic radiators given by equation 13.

---

[14]Shnitkin, _loc. cit._

Applying L'Hospital's rule, it can be shown that $|E_x| = 1.0$ when

$$\psi_x = \pm \, 2m\pi \, , \text{ where } m = 0, 1, 2 \ldots \, . \tag{33}$$

Also, it can be shown that $E_x = 0$ when

$$\frac{N\psi_x}{2} = \pm \, K\pi \, , \tag{34}$$

or

$$\psi_x = \pm \, \frac{2K\pi}{N} \quad .$$

where, because of equation 33, $K = 1, 2, 3, \ldots (N - 1)$. Hence, E_x has $N - 1$ zeroes as ψ_x varies from 0 to 2π, and $|E_x|$ reaches its maximum value when $\psi_x = 0$ and $\psi_x = 2\pi$.

In order that $|E_x|$ reach its maximum value only once as ψ_x varies through its range of values, a limitation must be placed upon the range of ψ_x. Shnitkin suggests that ψ_x be limited such that $|E_x|$ varies between its maximum value and its $(N - 1)$th zero. Thus, the grating lobe is eliminated when

$$\psi_x = 2\pi \, \frac{(N - 1)}{N} \quad . \tag{35}$$

In the ϕ-plane containing the array,

$$\psi_x = 2\pi d_\lambda \sin\Theta - 2\pi d_\lambda \sin\overline{\Theta} \leq \frac{2\pi\ (N-1)}{N} \qquad (36)$$

Hence

$$d_\lambda\ (max) = \frac{1 - (1/N)}{1 + \left|\sin\overline{\Theta}\right|} \qquad (37)$$

and d_λ (max) is the maximum spacing between elements of an N element linear array for a maximum scan angle $\overline{\Theta}$.

Figure 5 shows the spacing between elements or a function of the number of elements in one demension of an array for a maximum scan angle of 90° from broadside.
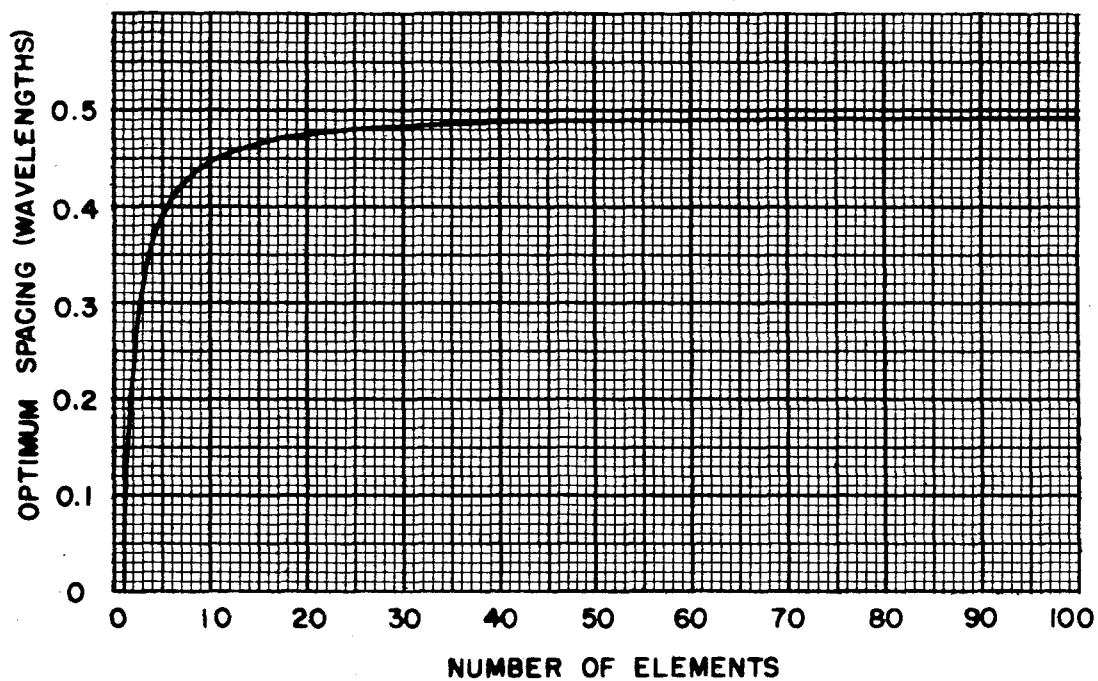
FIGURE 5   THE OPTIMUM SPACING FOR THE ELIMINATION OF THE
GRATING LOBE IN A SCANNED N x N ELEMENT ARRAY

III. EVALUATION OF THE MILLS CROSS AND THE TWO-DIMENSIONAL MATRIX ARRAY

In order to illustrate the shape of the radiation patterns of the two-dimensional matrix array and the effective beam patterns of the

$$F_\Theta = \frac{\sin (N\pi d_\lambda \sin \Theta \cos \phi + N \partial_x/2)}{N^2 \sin (\pi d_\lambda \sin \Theta \cos \phi + \partial_x/2)}$$

$$\frac{\sin (N\pi d_\lambda \sin \Theta \sin \phi + N\partial_y/2)}{\sin (\pi d_\lambda \sin \Theta \sin \phi + \partial_y/2)} \left[\frac{\cos^2 \Theta \sin^2 \phi \cos^2(\pi/2 \sin \Theta \sin \phi)}{(1 - \sin^2 \Theta \sin^2 \phi)^2} \right.$$

$$\left. + \frac{\cos^2 \phi \cos^2 (\pi/2 \sin \Theta \cos \phi)}{(1 - \sin^2 \Theta \cos^2 \phi)^2} \right]^{1/2} , \tag{38}$$

$$F_\phi = \frac{\sin (N\pi d_\lambda \sin \Theta \cos \phi + N\partial_x/2)}{N^2 \sin (\pi d_\lambda \sin \Theta \cos \phi + \partial_x/2)}$$

$$\frac{\sin (N\pi d_\lambda \sin \Theta \sin \phi + N\partial_y/2)}{\sin (\pi d_\lambda \sin \Theta \sin \phi + \partial_y/2)} \left[\frac{\cos^2 \phi \cos^2 (\pi/2 \sin \Theta \sin \phi)}{(1 - \sin^2 \Theta \sin^2 \phi)^2} \right.$$

$$\left. + \frac{\sin^2 \phi \cos^2 (\pi/2 \sin \Theta \cos \phi)}{(1 - \sin^2 \Theta \cos^2 \phi)^2} \right]^{1/2} . \tag{39}$$

The pattern factor components given by equations 38 and 39 are illustrated in Figures 1-A through 10-A in Appendix A for several values of N with the main beam pointing in the broadside direction. The main beam was found to have approximately a circular cross section in the broadside position so that only the patterns in the plane of $\phi = 0^{\circ}$ are shown for each value of N. In each case the element spacing was chosen to eliminate the grating lobe for a maximum scan angle of 90° from the broadside.

The crossed slot element has a radiation pattern in which the E_{θ}-component is constant and the E_{ϕ}-component is directional in the plane $\phi = 0$. Thus is Figures 1-A through 10-A, patterns of the E_{θ}-component may be considered as the patterns of an array of isotropic radiators, since the element does not affect the patterns. On the other hand, the patterns of the E_{ϕ}-component show the effect of the directional properties of the array element on the pattern factor of the array of isotropic radiators.

It was found that the side lobe level varies only slightly as a function of the number of elements. In Figure 1-A through 10-A, it may be seen that for the θ-component the maximum side lobe level varies between - 11.4db for N = 4 and - 13.5db for N = 100. The effect of the directive component of the antenna element is to reduce the side lobe level. The maximum side lobe level for the ϕ-component varies from - 18.9db for N = 4 to - 13.5db for N = 100.

Figure 6 shows the half-power beamwidth of the N x N element matrix array as a function of N both for the optimum spacing and for a
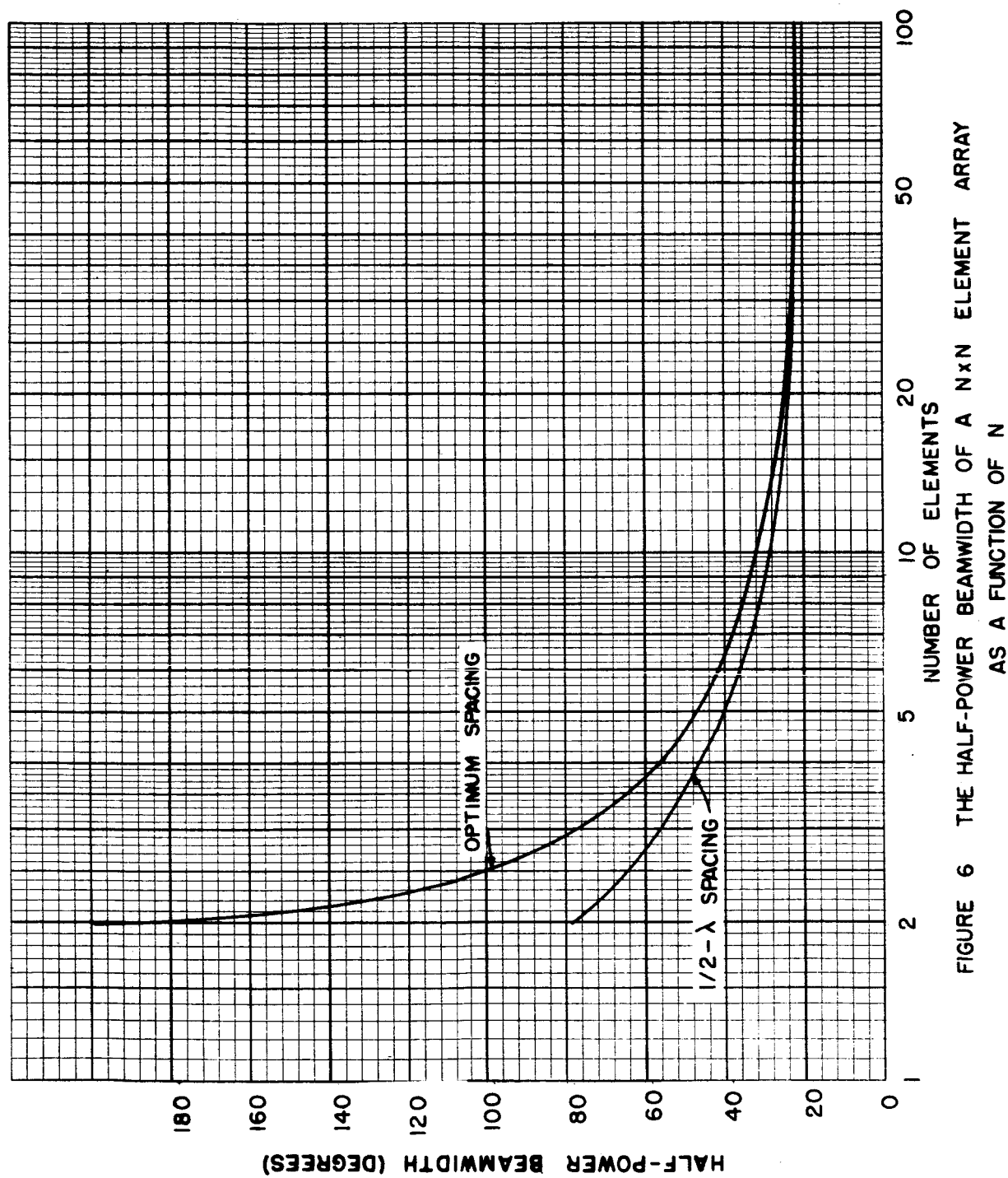
FIGURE 6   THE HALF-POWER BEAMWIDTH OF A N×N ELEMENT ARRAY
AS A FUNCTION OF N

constant one-half wavelength spacing. It is apparent that the optimum

spacing, which will eliminate the appearance of the grating lobe when

the beam is scanned, causes a broader beamwidth as compared to a

constant half wavelength spacing.

According to von Aulock[17], scanning the beam of a two-dimensional

array from the broadside direction does not affect the shape of the main

beam in the dimension perpendicular to the plane of scan. Thus, assuming

that all dimensions of the main beam are known in the broadside position,

it is sufficient to show the change of the beam shape in only one plane.

Figures 1-B through 6-B, in Appendix B, illustrate the effect of scanning

the beam on the radiation patterns of the array. These figures are for

the case of N = 5 and are shown in the plane of $\phi = 0$. It may be seen

that the beam shape is slightly changed for moderate scan angles but

that it is highly distorted for larger scan angles.

The effect of the directive component of the element factor is

apparent. As the scan angle increases, the element limits the array

pattern to the area enclosed by its own radiation pattern. For large

scan angles, the directive element component reduces the magnitude of

the beam maximum and introduces an error in the beam direction.

The maximum side lobe level of the E_Θ-component is found to be

constant as a function of scan angle. No large secondary or grating

lobes appear for any scan angle, and thus the optimum spacing is shown

to be valid. For the E_ϕ-component of the pattern, the maximum side

---

[17]Wilhelm H. von Aulock, "Properties of Phased Arrays," Proceedings
of the I.R.E., 48:1715-1727, October, 1960.

lobe level also remains constant with scan angle. However, if the side lobe level is expressed as decibels below the relative maximum of the component field pattern, the value of the level increases with scan angle.

The directivity of an antenna is defined as the ratio of the maximum radiation intensity to the average radiation intensity of the antenna under consideration[17]. The directivity, is descriptive of the radiation characteristics of the antenna and is used frequently to describe the ability of an antenna to direct its radiated energy in a particular direction. In the receiving sense, directivity provides a measure of the sensitivity of the antenna in a particular direction as compared to the sensitivity of the antenna in all other directions.

For the two-dimensional matrix antenna array, where the electric field intensity pattern is given by equation 27, the directivity is given by

$$D = \frac{4\pi r^2 P_{rm}}{W} ,$$
(40)

where W is the total power incident on the antenna, and P_{rm} is the value of the radial component of the average pointing vector in the direction in which it is a maximum[18]. Equation 40 may be reduced to

$$D = 4\pi/B$$
(41)

_____

[17]Kraus, op. cit., p. 27.

[18]Ibid., pp. 23-25.

where B is the beam area, defined as the solid angle through which all the power radiated by the antenna would flow if the power per unit solid angle equaled the maximum value over the beam area[19].

Equation 41 yields an exact value of the directivity of an antenna. An approximate value may be obtained by estimating the beam area. For single lobed radiation patterns, a close approximation of the beam area can be made from the half-power beamwidths in two orthogonal planes. If Θ_0 is the beam width between half-power points in one plane and ϕ_0 is the half-power beamwidth in a perpendicular plane, the beam is approximately[20]

$$B = \Theta_0 \phi_0 \quad , \tag{42}$$

where Θ_0 and ϕ_0 are expressed in radians. Substituting this approximate expression in equation 41

$$D = \frac{4\pi}{\Theta_0 \phi_0} \quad . \tag{43}$$

The approximation was based on a single lobed antenna pattern and will continue to hold for unidirectional antenna patterns where the side lobe level is low.

Figure 7 illustrates the change in directivity as a function of scan angle for the N x N matrix array and the effective beam of the Mills cross array. The directivity was found by using equation 43. The ϕ_0 in
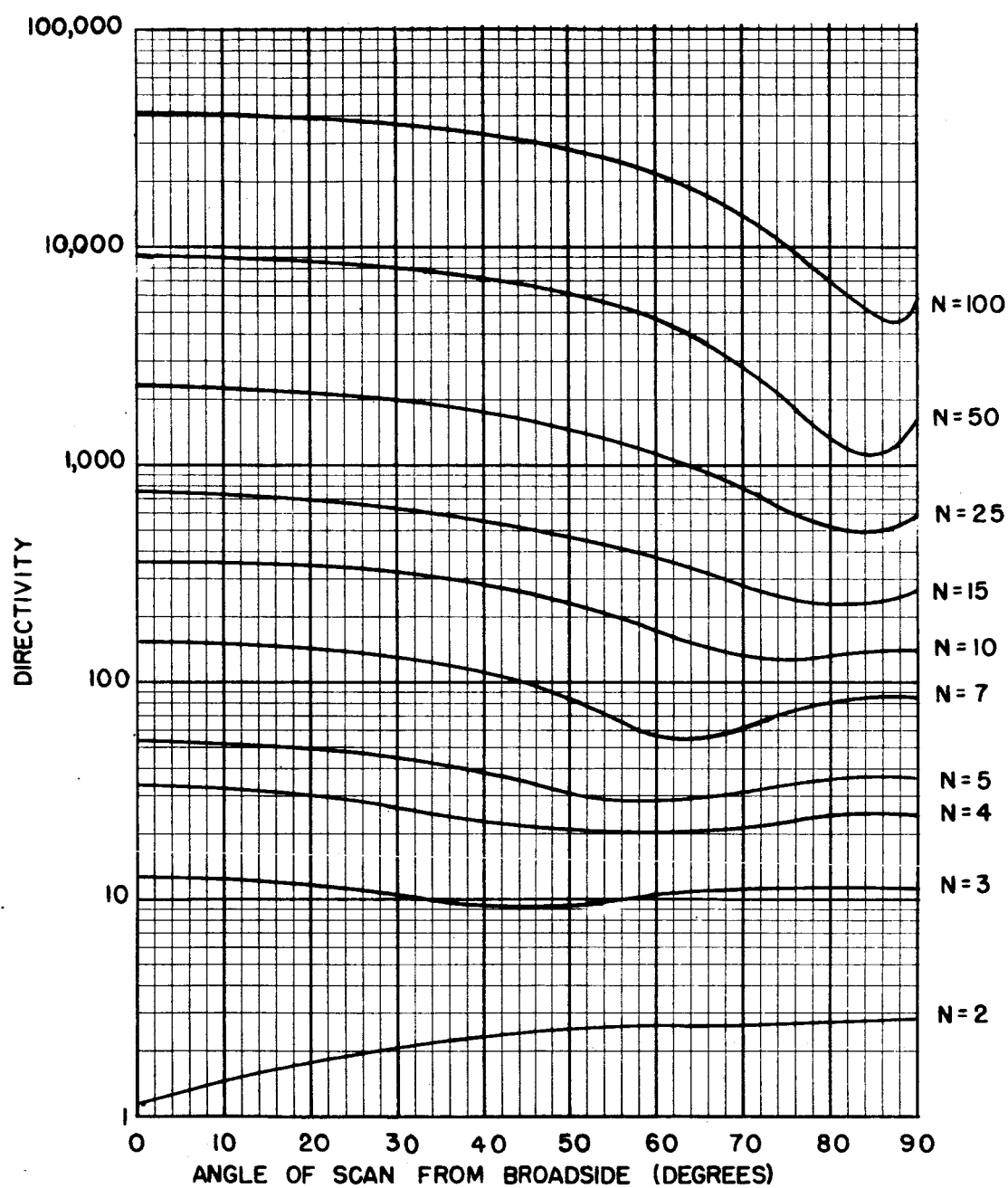
[19]Ibid., p. 25.

[20]Ibid.

FIGURE 7- THE DIRECTIVITY OF THE N x N ELEMENT ARRAY AS A FUNCTION OF SCAN ANGLE

equation 43 was assumed to be the half power beamwidth in the $\phi = 90°$ plane when the beam was in the broadside position. Θ_0 in equation 43 was calculated in the plane $\phi = 0°$, which is the plane of scan. The Θ_0 was assumed to be the angle between the half-power points when two half-power points were defined, or otherwise the angle between the half-power point and the x-axis. This definition of Θ_0 accounts for the deviations in the curves of Figure 7 and indicates the distortion in the beam shape for large scan angles.

The directivity, as defined in equation 43 is not entirely valid for the Mills cross array. It is, however, indicative of the resolution of the array and shows the utility of the array in directional applications.

Ksienski[21] suggests a method of determining the efficiency of the Mills cross array. Since the directionality of the array is achieved by rejecting in the processing stage the majority of the energy received by the array, the efficiency may be represented by the ratio of the total energy received to the energy contained in the intersection beam.

An approximate representation of the directivity of a Mills cross array may be determined by applying a technique similar to that above. An effectiveness ratio may be defined as the ratio of the beam array in the intersection of the fan beams to the total beam area of the two beams. Employing the same approximation for the beam area as was used in equation 43, the effectiveness ratio may be written as

---

[21]Ksienski, op. cit., p. 79.

$$\alpha = \frac{\Theta_0 \phi_0}{\Theta_0 B_0 + \phi_0 \gamma_0} \qquad (44)$$

where Θ_0 and ϕ_0 are the half-power beamwidths in the narrow dimensions of the two fan beams, and B_0 and γ_0 are the half-power beamwidghs in the wide dimension of the fan beams. If the two fan beams are identical, equation 44 reduces to

$$\alpha = \frac{\Theta_0}{2B_0} \quad . \qquad (45)$$

Equation 43 may be used to find the directivity of the two fan beams. Thus,

$$D = \frac{2\pi}{\Theta_0 B_0} \quad . \qquad (46)$$

By combining equations 45 and 46, the effective directivity of the Mills cross array is obtained and is given by

$$D_\eta = \frac{\pi}{B_0^2} \quad . \qquad (47)$$

Since, for a given array element, B_0 is a constant, the effective directivity is also a constant and does not depend upon the number of elements in the array.

IV. CONCLUSIONS

The Mills cross antenna array of 2N elements has been shown to have an effective radiation pattern which is equivalent to that of the two-dimensional matrix antenna array having N^2 elements. The patterns of the two antenna arrays are presented for several sizes of arrays. The directivity, which was approximated by using the dimensions of the effective beam patterns, was found to increase rapidly with the size of the array. Although the directivity, which was calculated from the pattern dimensions, is indicative of the resolution properties of the Mills cross array, it is also a valid representation of the directivity of the matrix array and is proportional to the gain of that array. Another expression was developed which more accurately approximates the overall directivity of the Mills cross array. This effective directivity was found to be constant, indicating that the gain of the array remains low, independent of the size of the array.

The Mills cross array has a obvious advantage over the matrix array in that the number of elements required to produce a certain beamwidth is considerably less for the Mills cross array. However, this advantage is almost overshadowed by the fact that the Mills cross can only be used in specialized applications. Becuase of the manner in which the signal is processed to produce the effective narrow beam, the antenna array cannot be assumed to have reciprocal properties. Thus, the array can only be used to receive continuous-wave radio-frequency signals such as the energy from a radio star or an r-f beacon from a

satellite. In the special applications where the Mills cross may be used, the gain of the antenna is usually not of primary interest but rather the resolution or the ability to distinguish between two closely spaced point targets is the important factor. Again it may be emphasized that the Mills cross has the same degree of resolution as the larger array of N/2 times more elements.

Although no particular circuit or scheme was presented by which the beam of the two arrays might be scanned, it is obvious that any one of several techniques may be employed to provide a variable differential phase shift between the array elements. The phase shift may be made in given increments by using digital techniques, or it may be made continuously by using analogue techniques. In any event, it is apparent that with every element of the array there is associated at least one phase-shifting device. Hence the advantages of reducing the number of elements are at least doubled when the accompanying components are considered.

It has been shown that the possibility exists for scanning the beam of the arrays through-out the hemisphere. The shape of the beam was shown to change slightly for moderate scan angles and more drastically for greater scan angles near end-fire. An optimum spacing was employed which eliminated the appearance of grating lobes in the radiation patterns as the beam was scanned. Even though the grating lobes were eliminated, no reduction in side lobe level was obtained. However several schemes of side lobe reduction are presented in the literature[22] which could be applied to either of the two arrays.

[22]C. L. Dolph, "A Current Distribution for Broadside Arrays Which Optimizes the Relationship Between Beamwidth and Side-Lobe Level," Proceedings of the I.R.E., 34:335-348, June, 1946.

BIBLIOGRAPHY

BIBLIOGRAPHY

Brown, G. H., "The Turnstile Antenna," *Electronics*, 9:14-17,48, April. 1936.

Dolph, C. L., "A Current Distribution for Broadside Arrays Which Optimizes the Relationship Between Beamwidth and Side-Lobe Level," *Proceedings of the I.R.E.*, 34:335-348, June, 1946.

Fradin, A. Z., *Microwave Antennas*, New York: Pergamon Press, 1961.

Jasik, Henry (ed.), *Antenna Engineering Handbook*, New York: McGraw-Hill Book Co., 1961.

Kraus, John D., *Antennas*, New York: McGraw-Hill Book Co., 1950.

Ksienski, A., "Signal Processing Antennas - Part I," *Microwave Journal*, 4:77-85, October, 1961.

Landee, Robert W., Donavan C. Davis and Albert P. Albrecht, *Electronic Designer's Handbook*, New York: McGraw-Hill Book Company, 1957.

Lewis, Walter W. and Clarance F. Goodhart, *Basic Electric Circuit Theory*, New York: The Ronald Press Company, 1958.

Mills, B. Y. and A. G. Little, "A High-resolution aerial system of a new type," *Australian Journal of Physics*, 6:272-278, September, 1953.

Mills, B. Y., and others, "A High Resolution Radio Telescope for use at 3.5 meters," *Proceedings of the I.R.E.*, 46:67-84, January, 1958.

Shnitkin, Harold, "A Survey of Electronically Scanned Antennas - Part I," *Microwave Journal*, 3:67-72, October, 1960.

von Aulock, Wilhelm H., "Properties of Phased Arrays," *Proceedings of the I.R.E.*, 48:1715-1727, October, 1960.

APPENDIX A

The Normalized Field Patterns of the N x N Element Matrix Array in the plane of $\phi = 0$ are as follows:

$\dfrac{E}{E_m}$

1.0

θ

0.5

E_θ- COMPONENT

$\dfrac{E}{E_m}$

1.0

θ

0.5

E_ϕ- COMPONENT
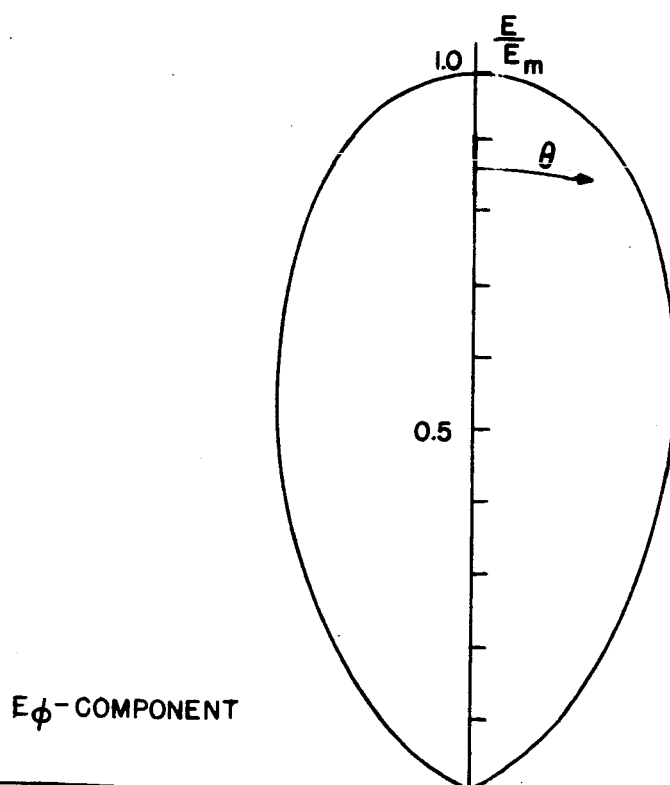
FIGURE A-I   THE NORMALIZED FIELD PATTERNS OF THE N x N   ELEMENT
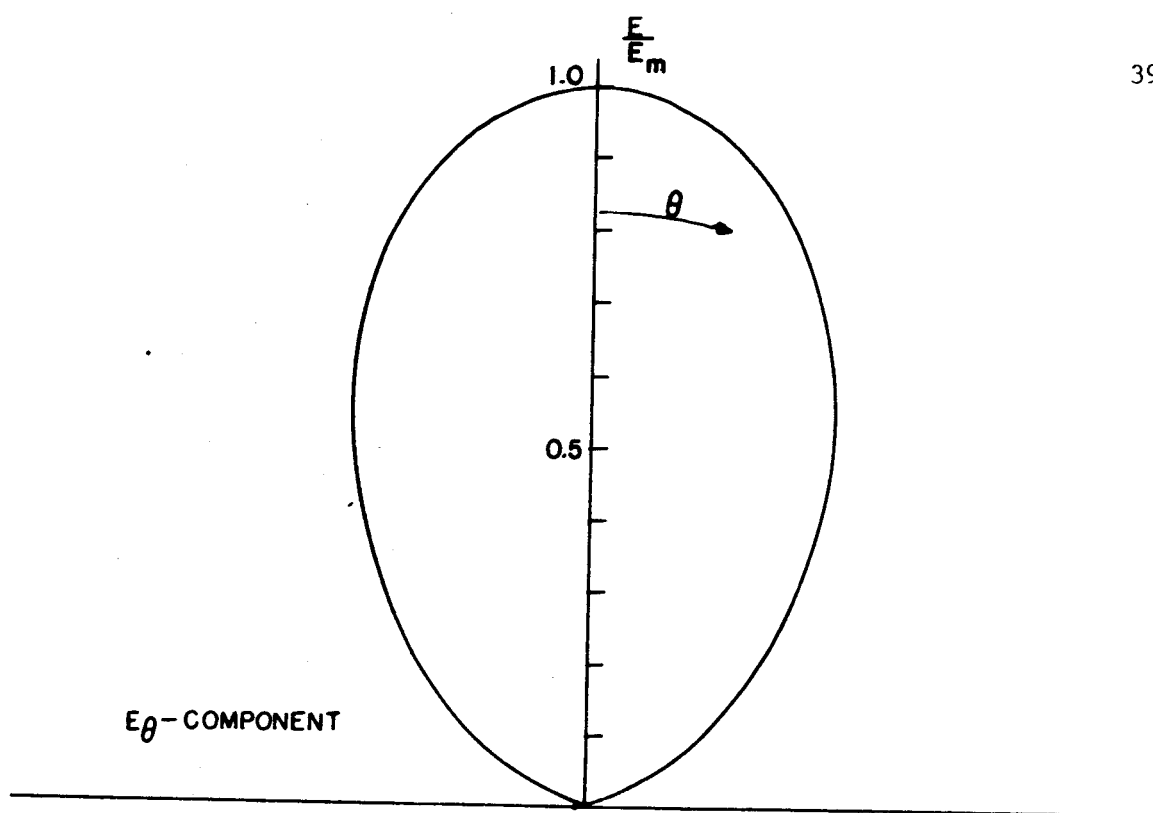MATRIX ARRAY   (N=2)

$\frac{E}{E_m}$

1.0

0.5

θ

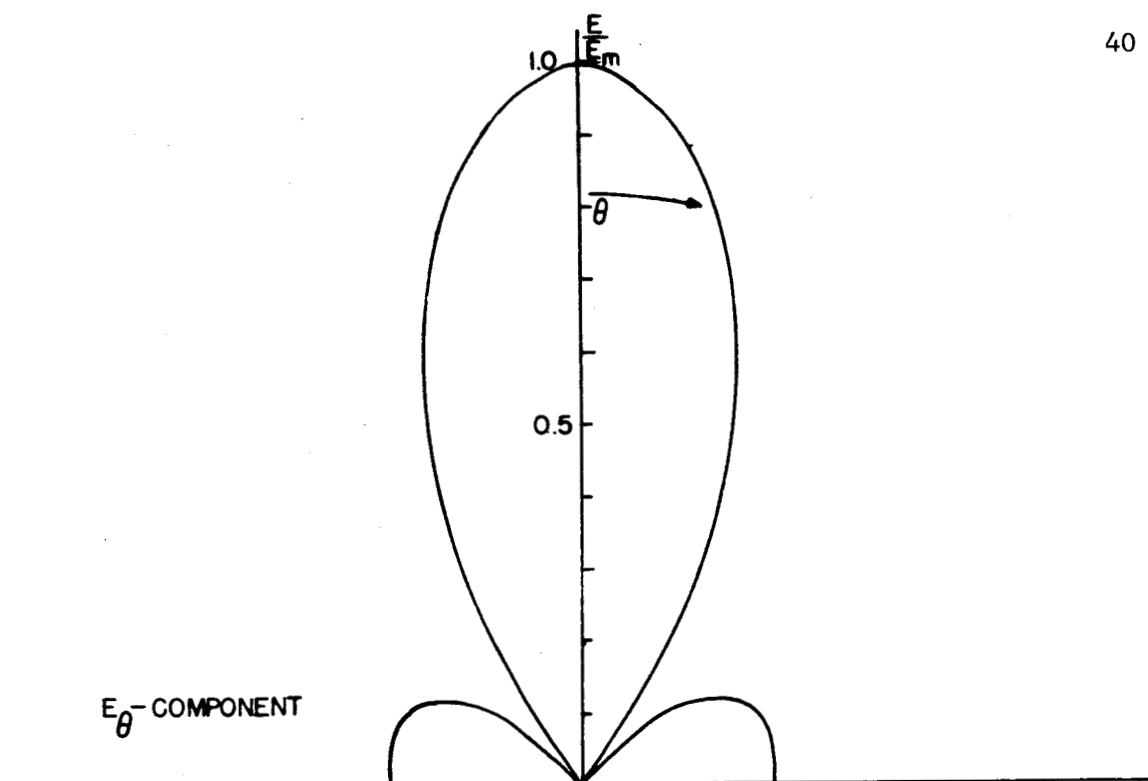E_θ - COMPONENT
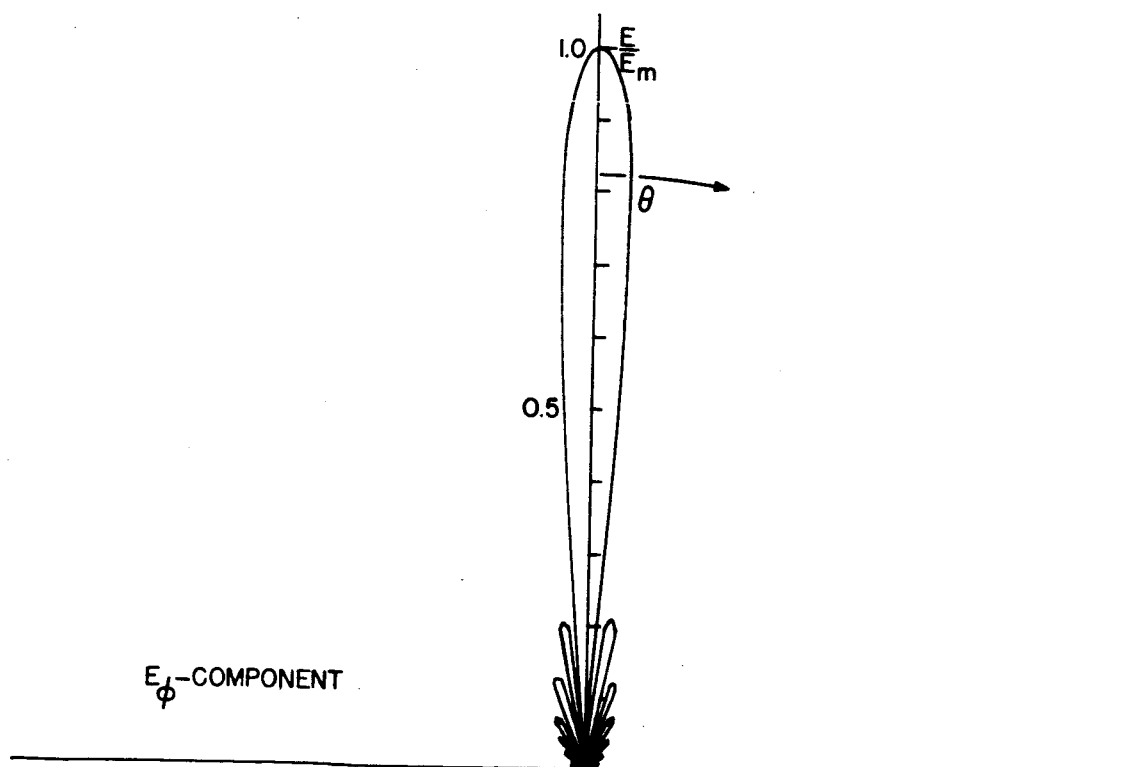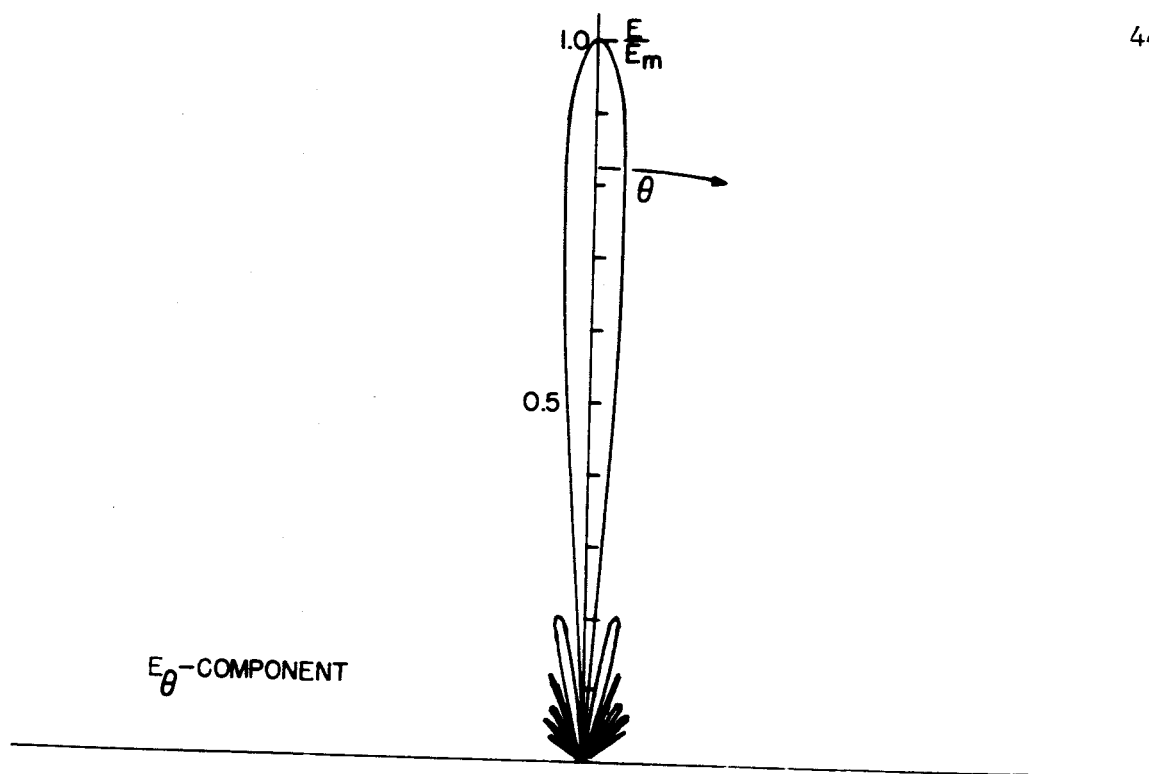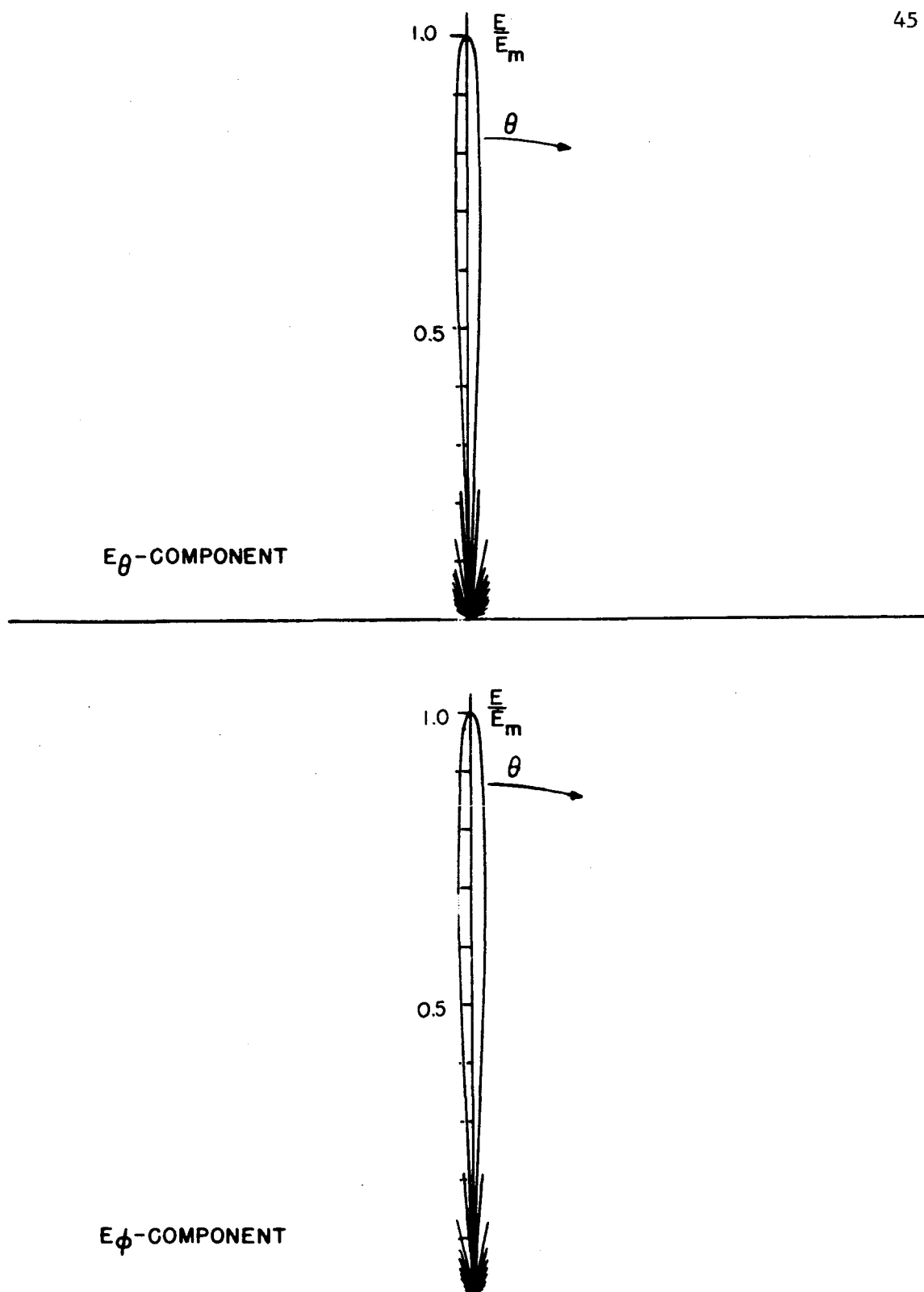
$\frac{E}{E_m}$

1.0

0.5

θ

E_ϕ - COMPONENT

FIGURE A-2 THE NORMALIZED FIELD PATTERNS OF THE N x N ELEMENT MATRIX ARRAY (N = 3)
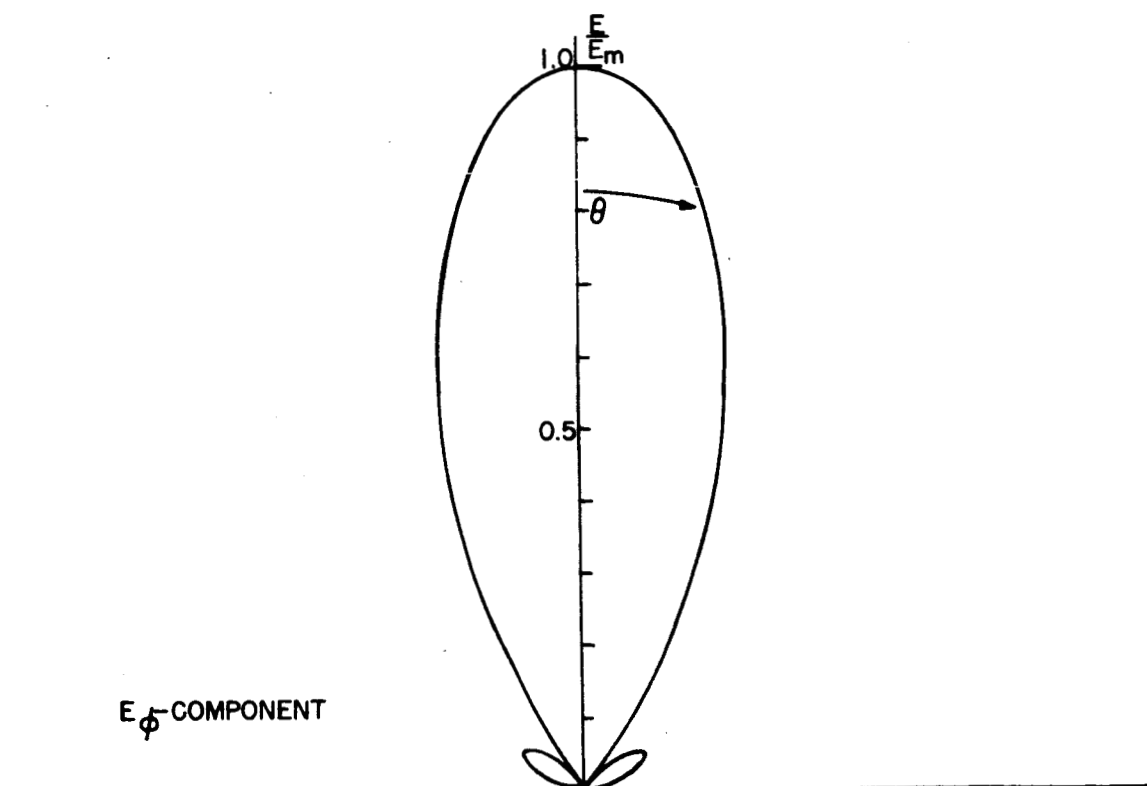
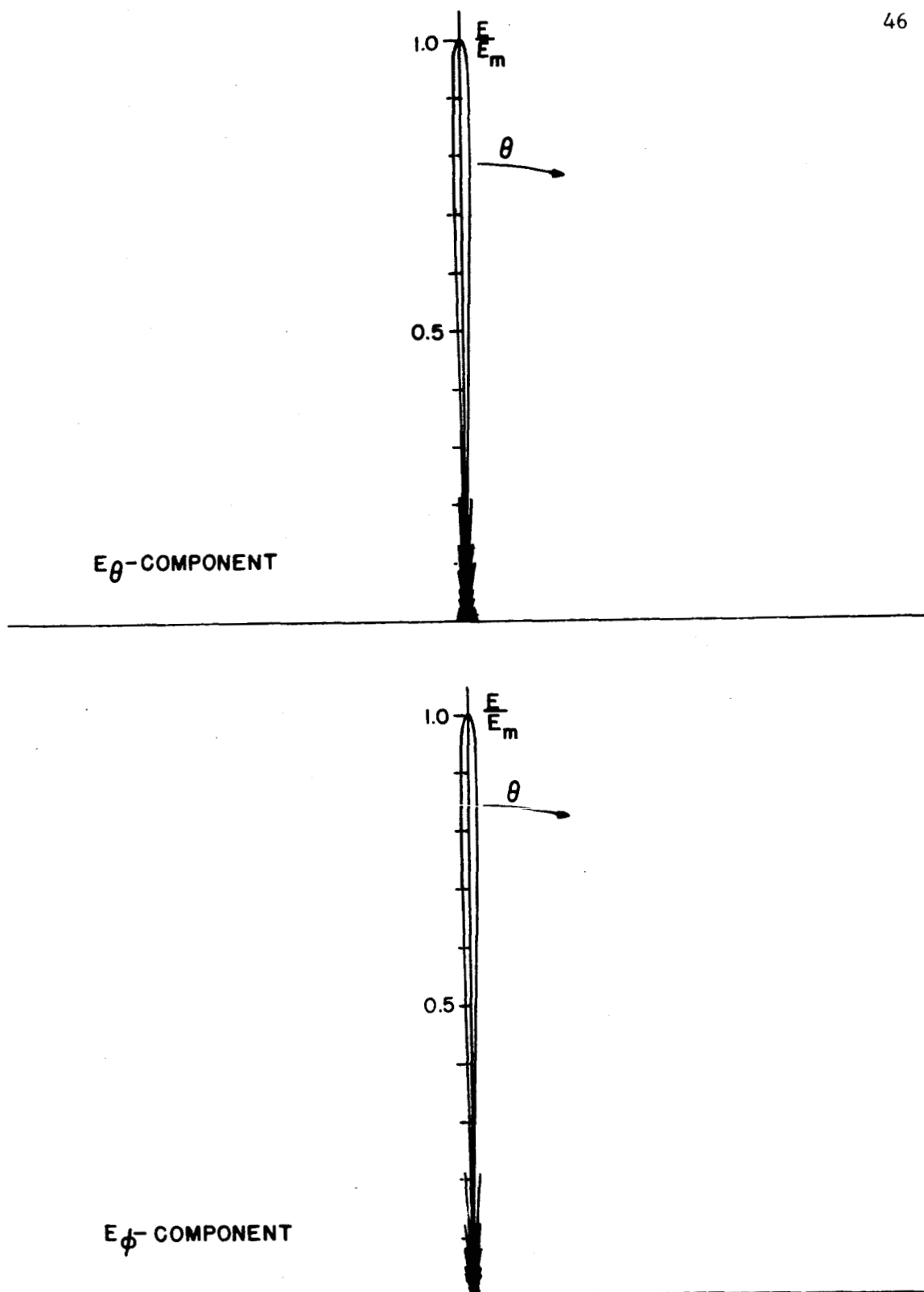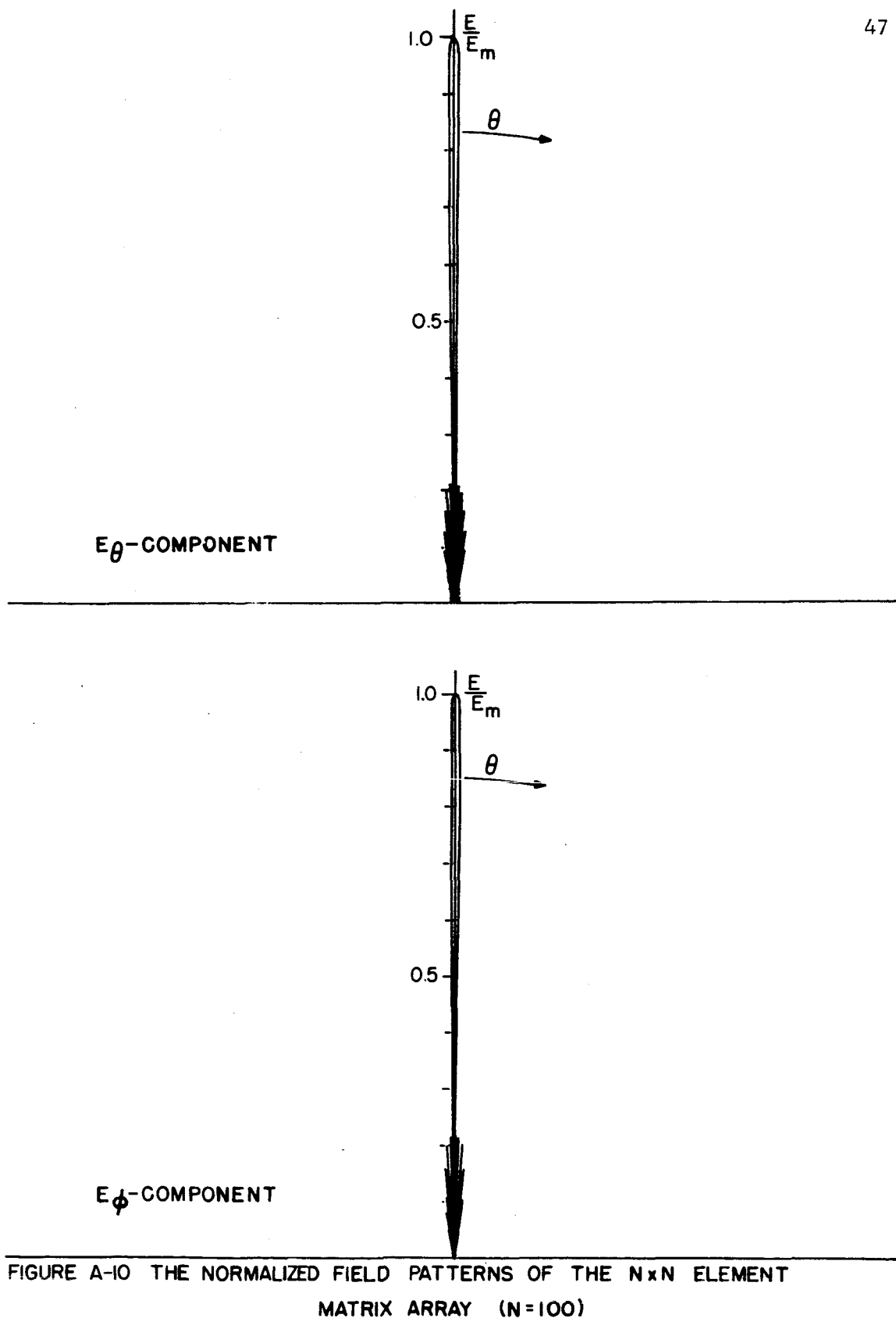FIGURE A-3   THE NORMALIZED FIELD PATTERNS OF THE N x N ELEMENT
MATRIX ARRAY (N=4)

$\frac{E}{E_m}$

1.0

θ

0.5

E_θ-COMPONENT

$\frac{E}{E_m}$

1.0

θ

0.5

E_ϕ-COMPONENT
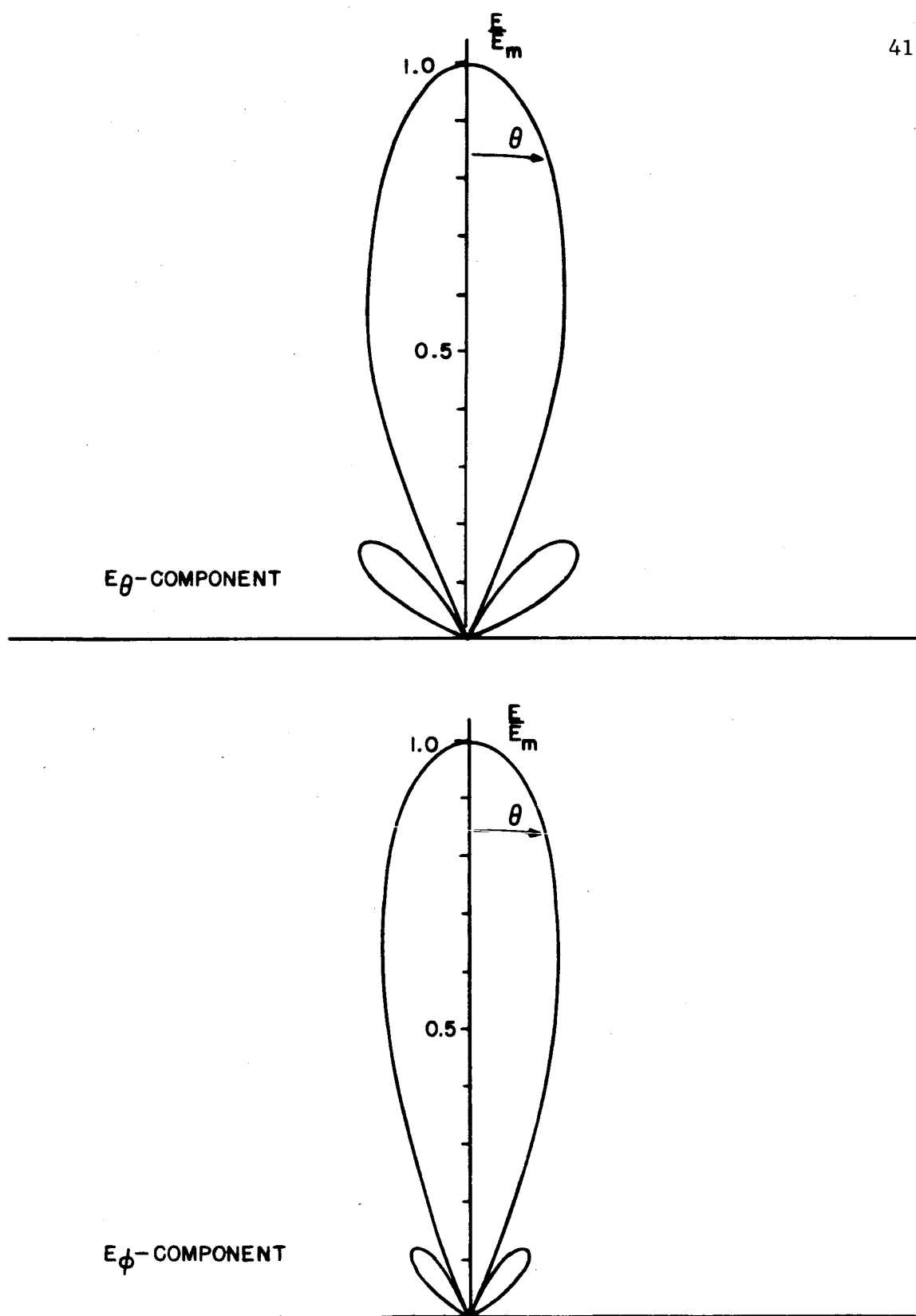
FIGURE A-4 THE NORMALIZED FIELD PATTERNS OF THE N x N ELEMENT

MATRIX ARRAY (N = 5)

E_θ-COMPONENT

E_ϕ-COMPONENT

FIGURE A-5 THE NORMALIZED FIELD PATTERNS OF THE N×N ELEMENT
MATRIX ARRAY (N=7)

$$\frac{E}{E_m}$$

1.0

0.5

θ

E_θ—COMPONENT

$$\frac{E}{E_m}$$

1.0

0.5

θ

E_ϕ—COMPONENT
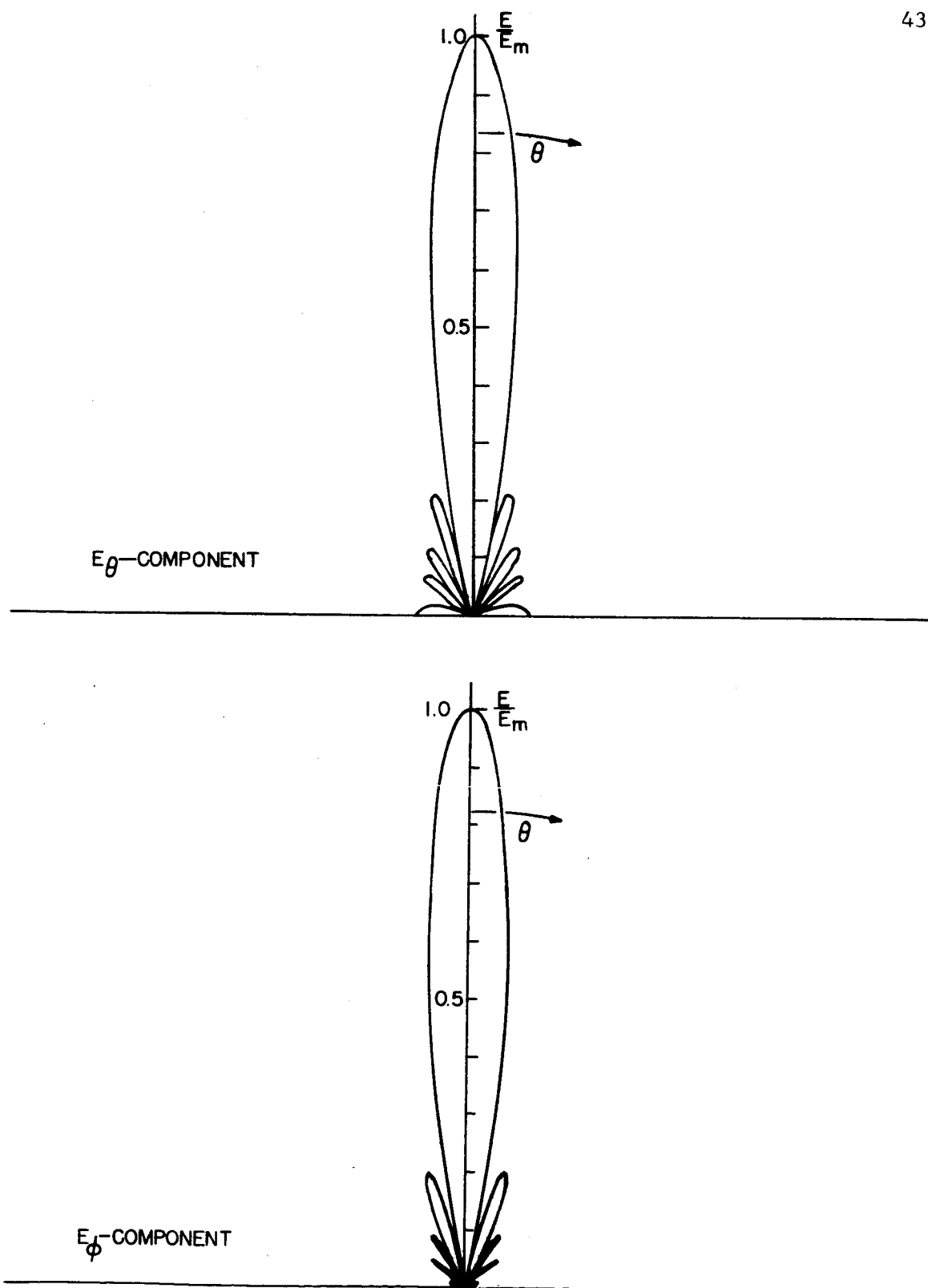
FIGURE A-6 THE NORMALIZED FIELD PATTERNS OF THE NxN ELEMENT
MATRIX ARRAY (N=IO)

E_θ-COMPONENT

E_ϕ-COMPONENT

FIGURE A-7   THE NORMALIZED FIELD PATTERNS OF THE N x N ELEMENT
MATRIX ARRAY (N=15)

$\dfrac{E}{E_m}$

1.0

θ

0.5

E_θ-COMPONENT

$\dfrac{E}{E_m}$

1.0

θ

0.5

E_ϕ-COMPONENT

FIGURE A-8   THE NORMALIZED FIELD PATTERNS OF THE N x N   ELEMENT
MATRIX ARRAY   (N = 25)

E_θ-COMPONENT

E_ϕ- COMPONENT

FIGURE A-9 THE NORMALIZED FIELD PATTERNS OF THE N x N ELEMENT

MATRIX ARRAY (N = 50)

$\dfrac{E}{E_m}$

1.0

θ

0.5

E_θ-COMPONENT

$\dfrac{E}{E_m}$

1.0

θ

0.5

E_ϕ-COMPONENT

FIGURE A-10 THE NORMALIZED FIELD PATTERNS OF THE N x N ELEMENT
MATRIX ARRAY (N = 100)

APPENDIX B

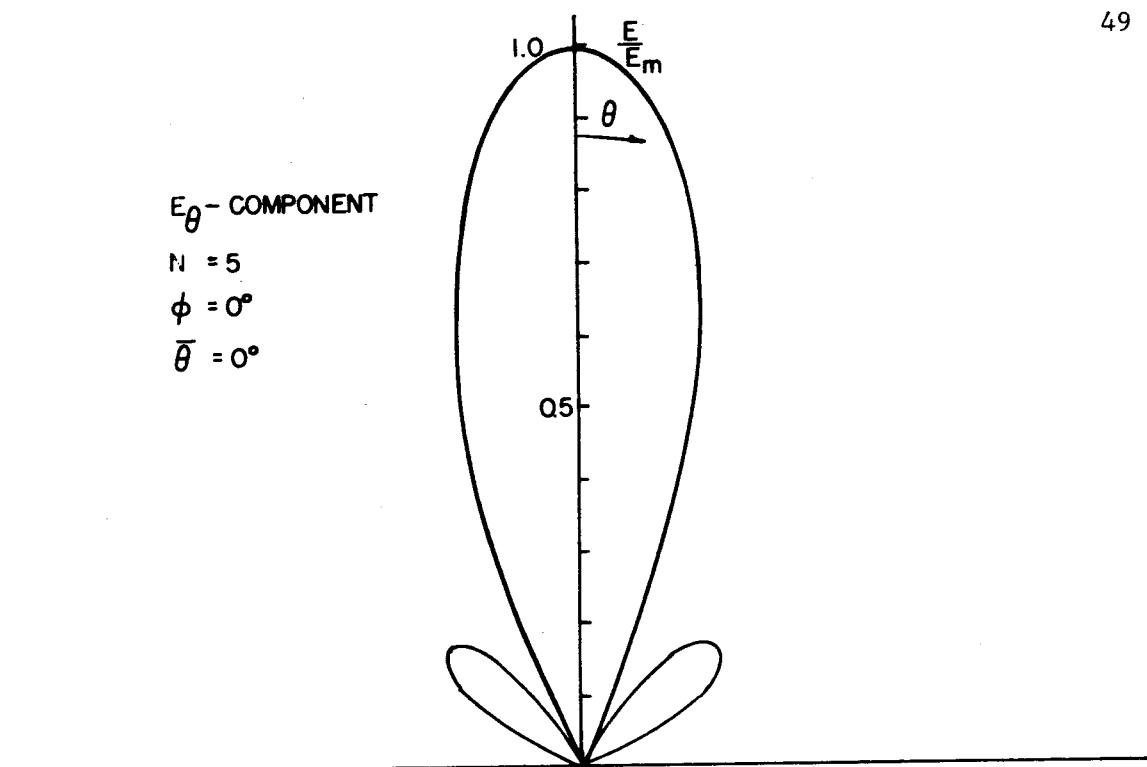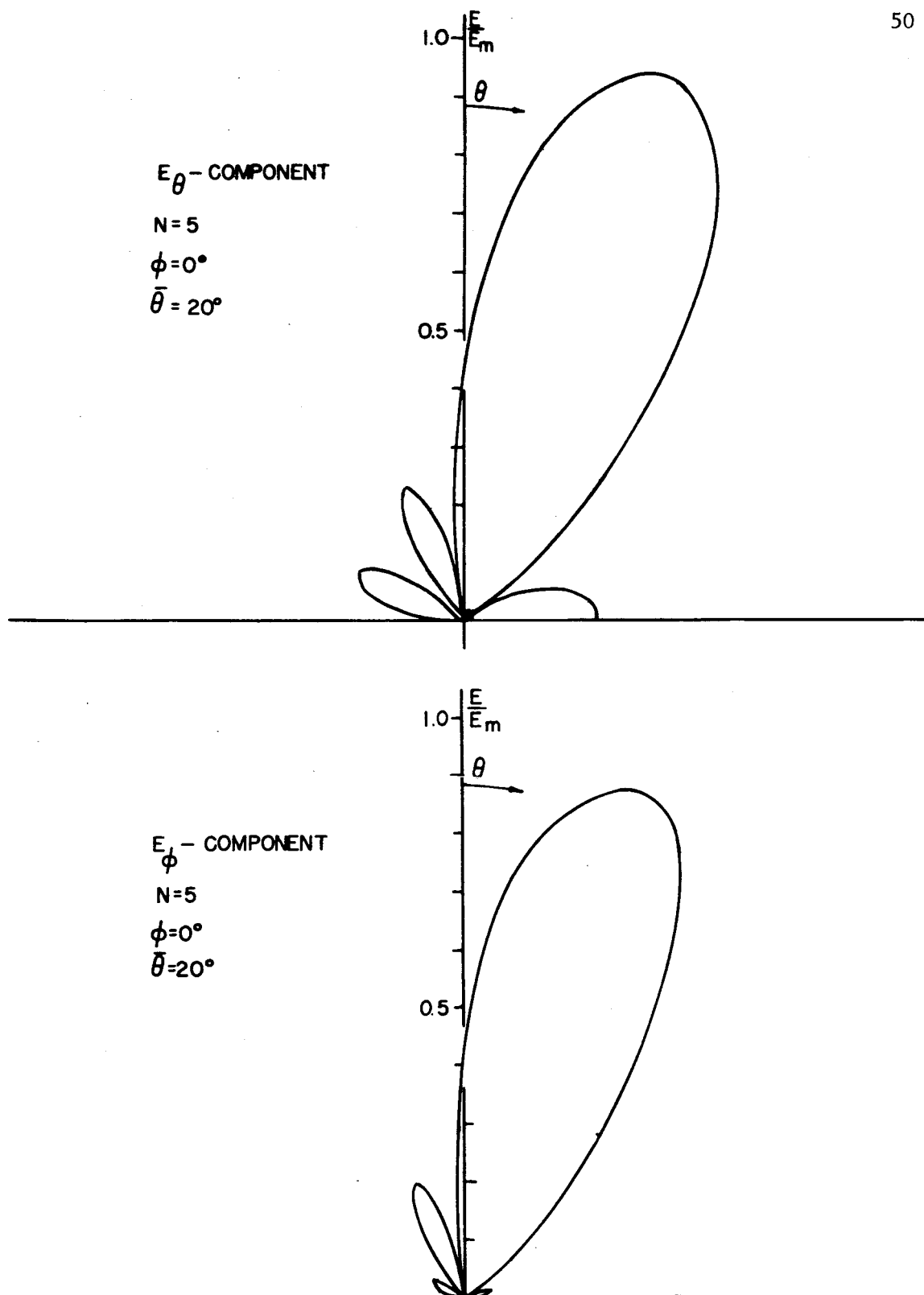The Normalized Field Patterns of the Matrix Array of crossed slot antennas illustrating the effect of beam scanning are presented as follows:
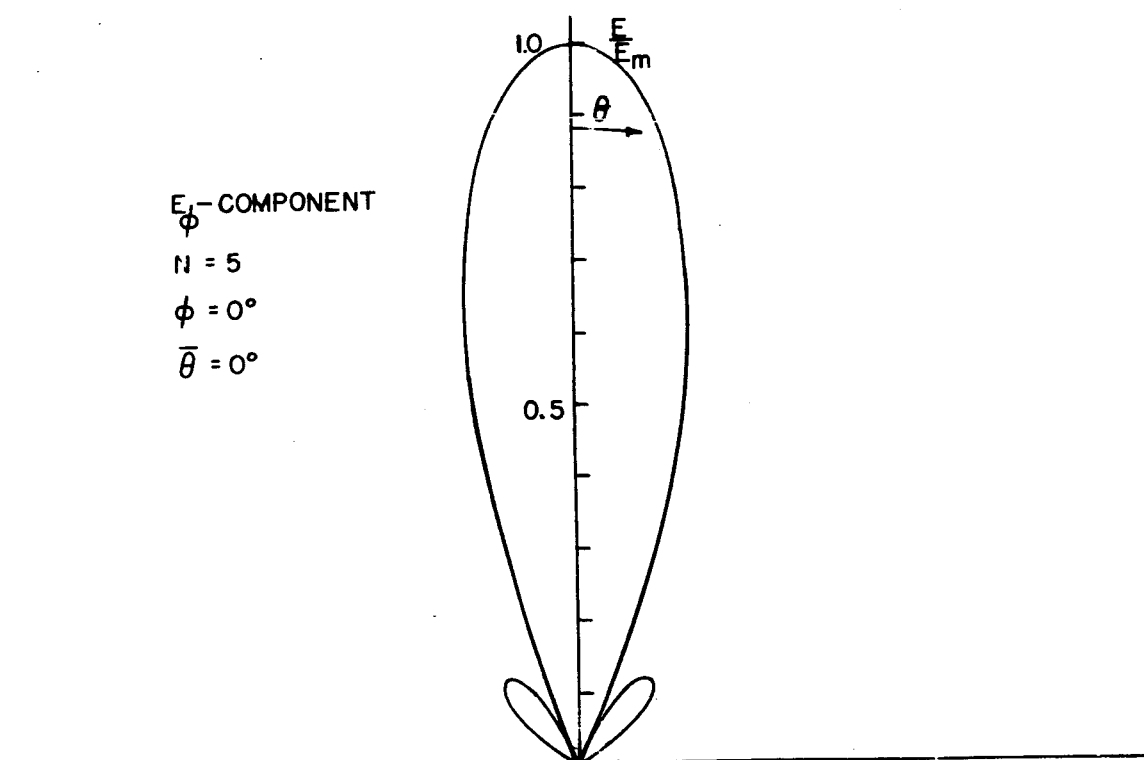
E_θ - COMPONENT

N = 5

$\phi = 0°$

$\overline{\theta} = 0°$

E_ϕ - COMPONENT

N = 5

$\phi = 0°$
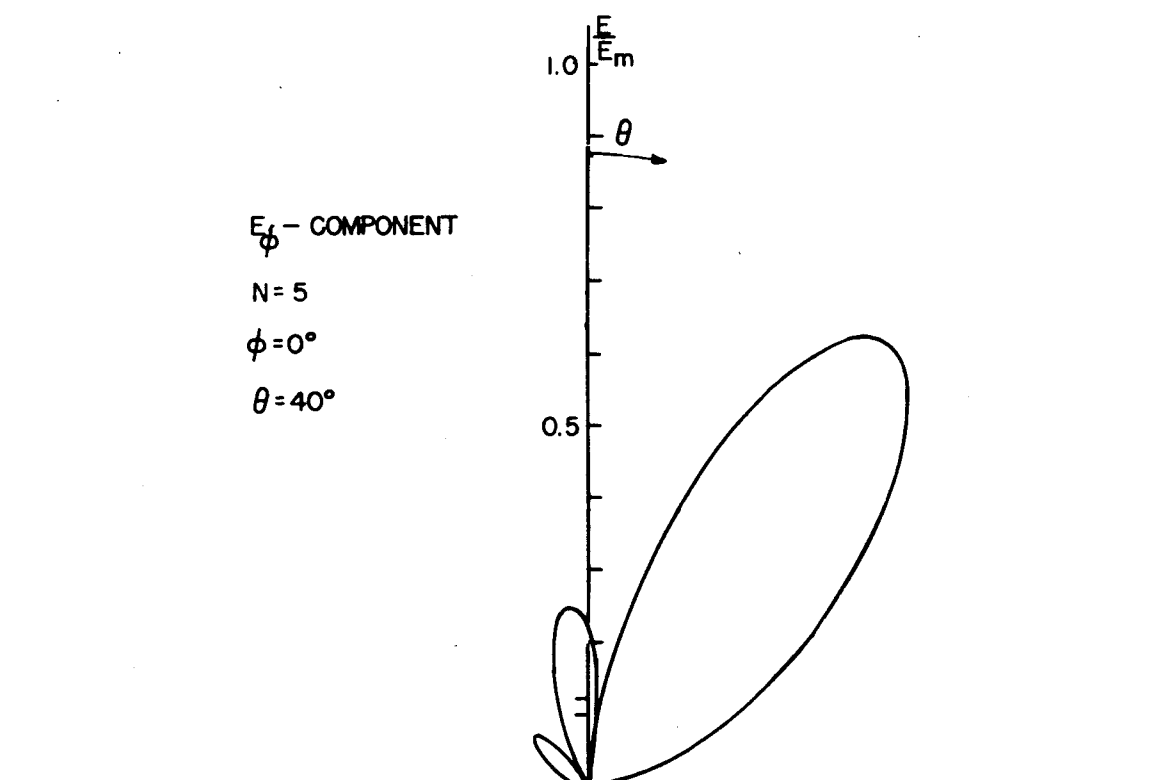
$\overline{\theta} = 0°$

FIGURE B-I THE NORMALIZED FIELD PATTERN OF THE MATRIX ARRAY OF CROSSED
SLOT ANTENNAS ILLUSTRATING EFFECT OF BEAM SCANNING

FIGURE B-2 THE NORMALIZED FIELD PATTERN OF THE MATRIX ARRAY OF CROSSED
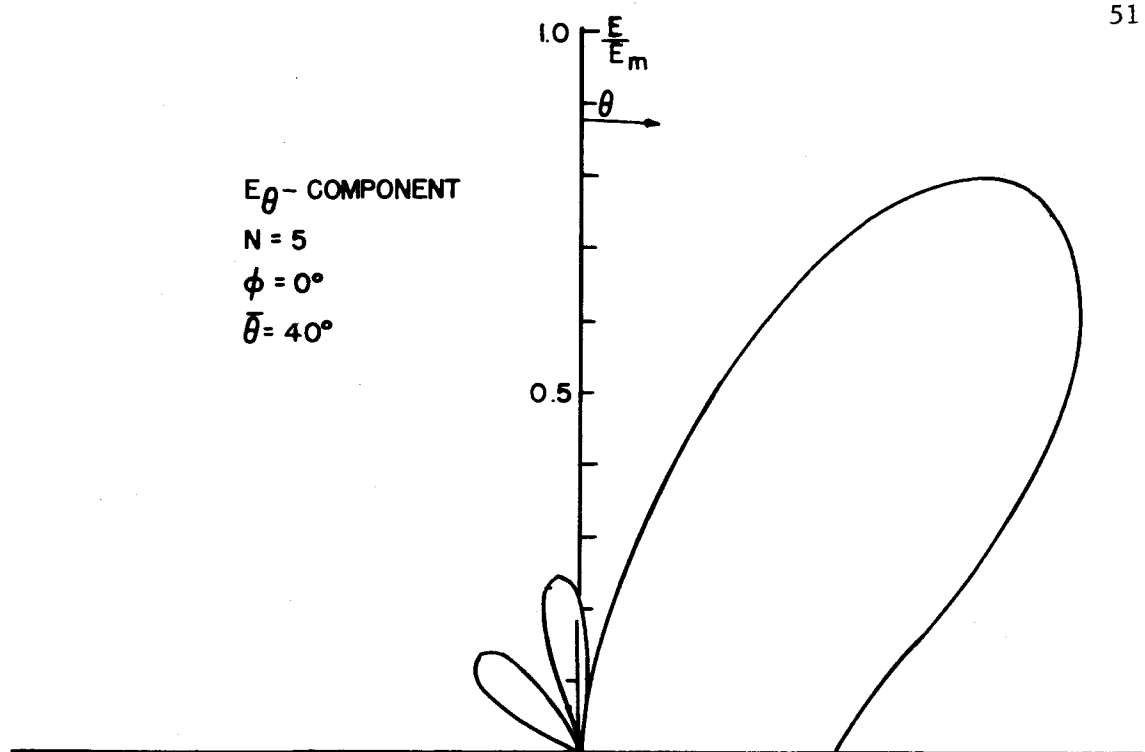SLOT ANTENNAS ILLUSTRATING EFFECT OF BEAM SCANNING

FIGURE B-3 THE NORMALIZED FIELD PATTERN OF THE MATRIX ARRAY OF CROSSED
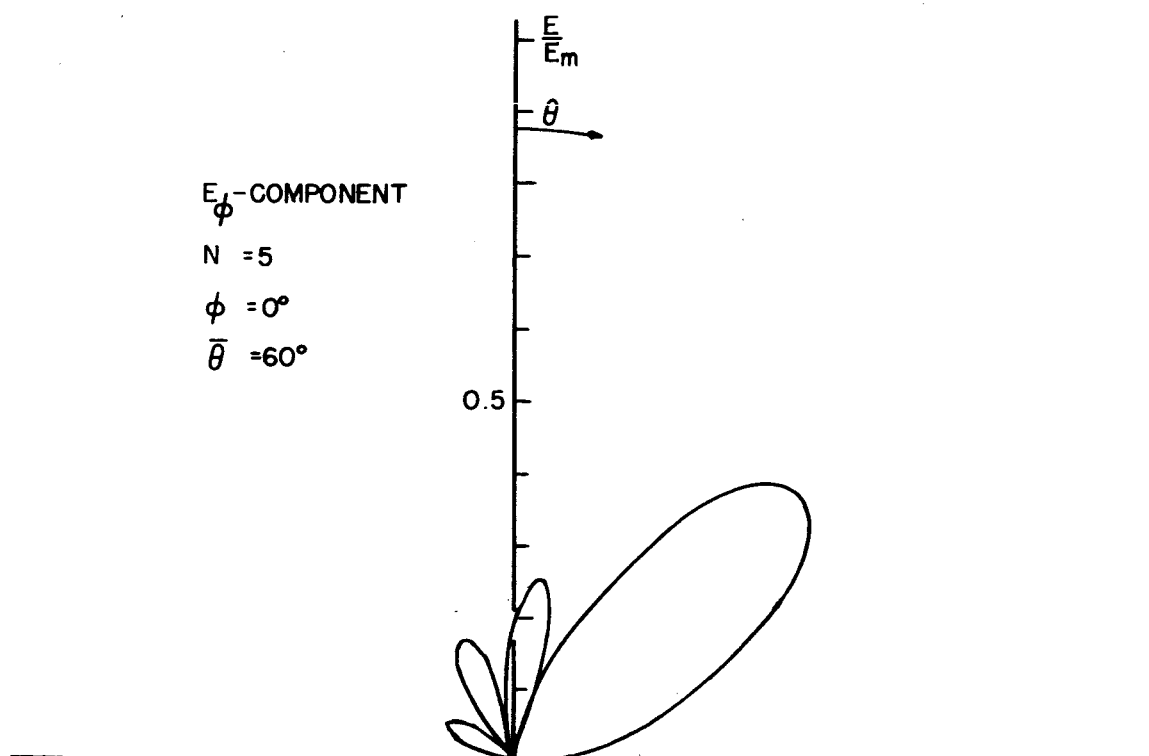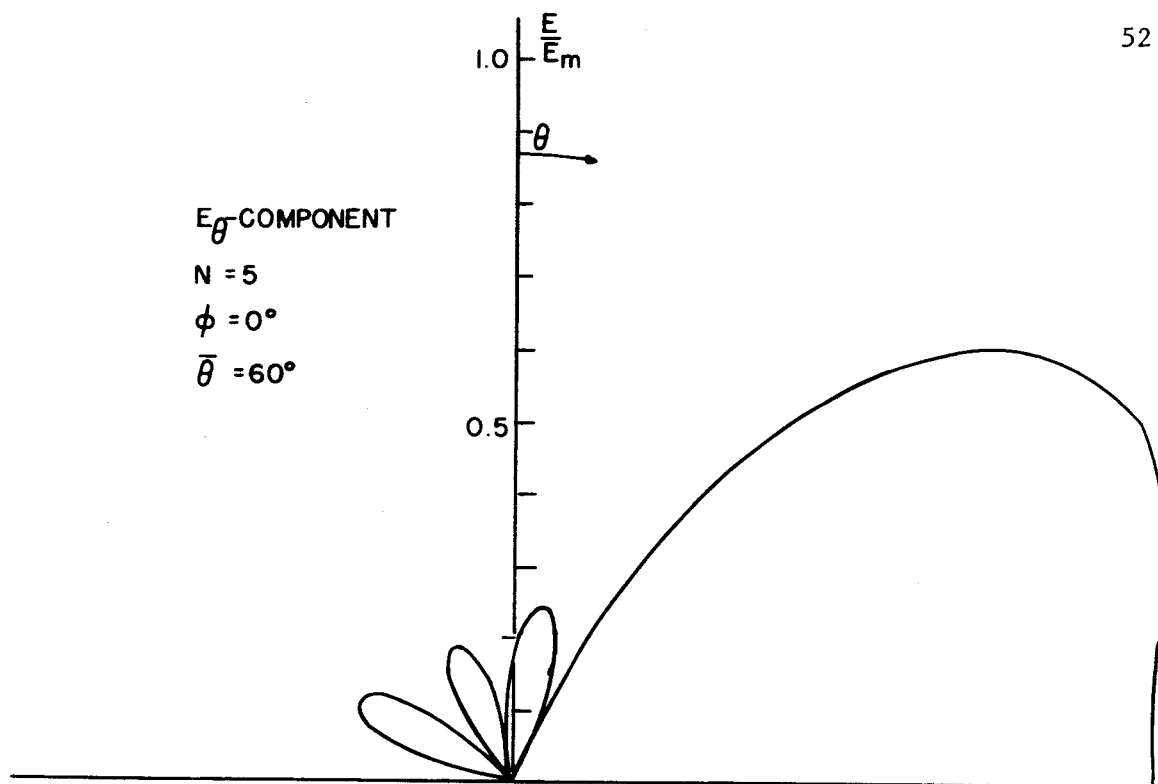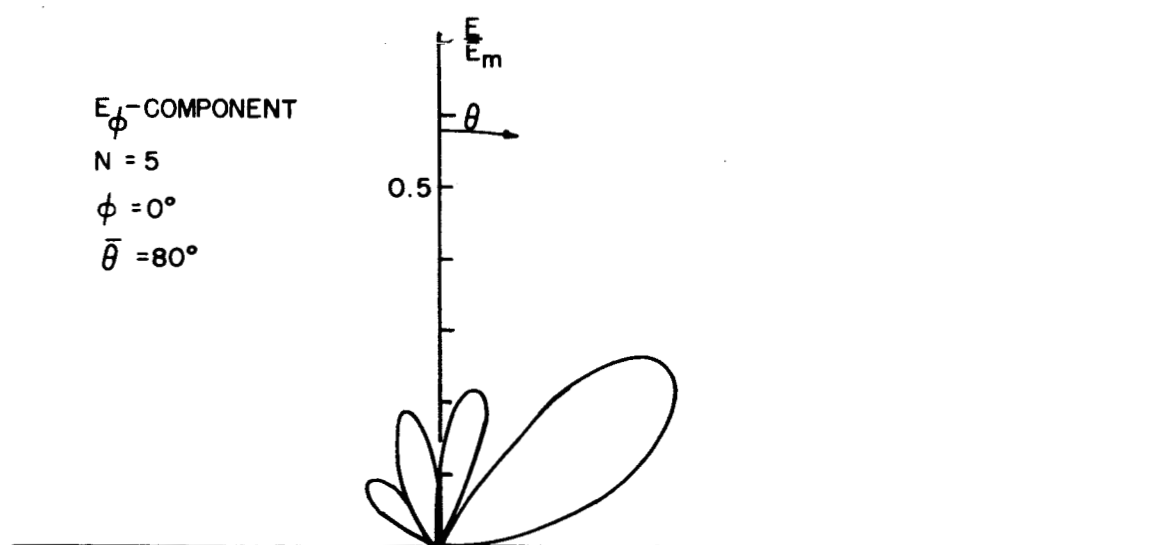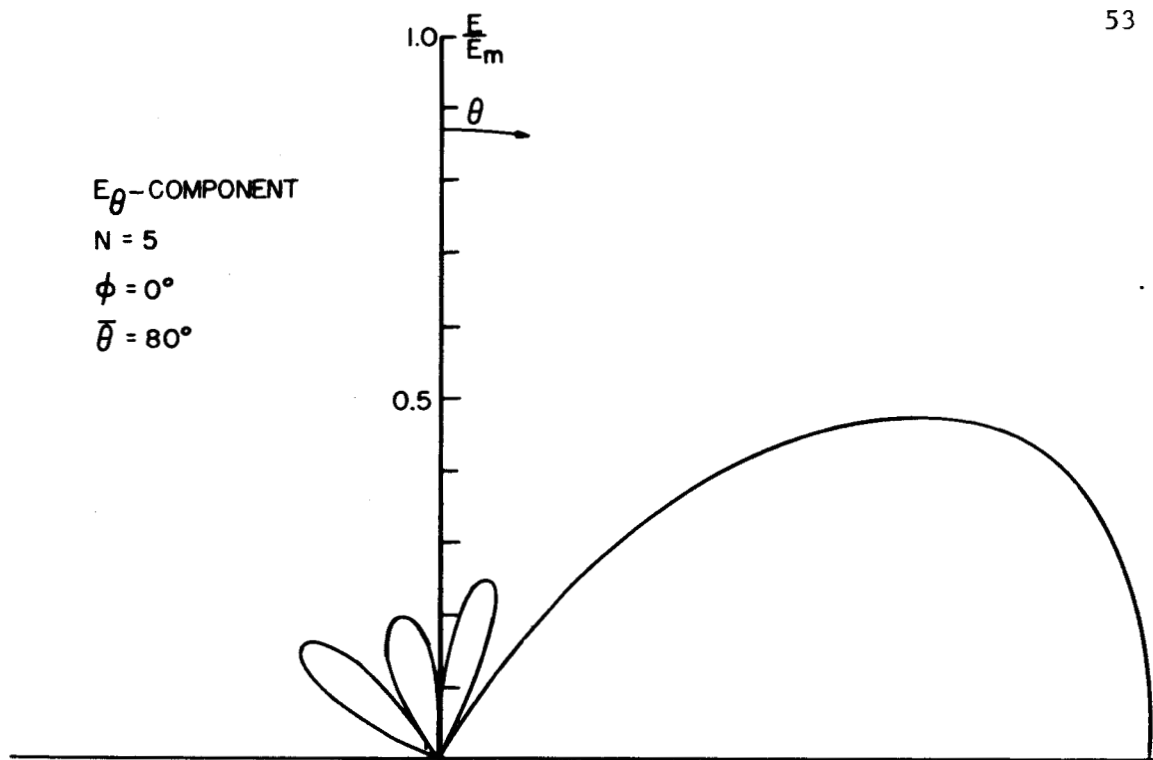SLOT ANTENNAS ILLUSTRATING EFFECT OF BEAM SCANNING
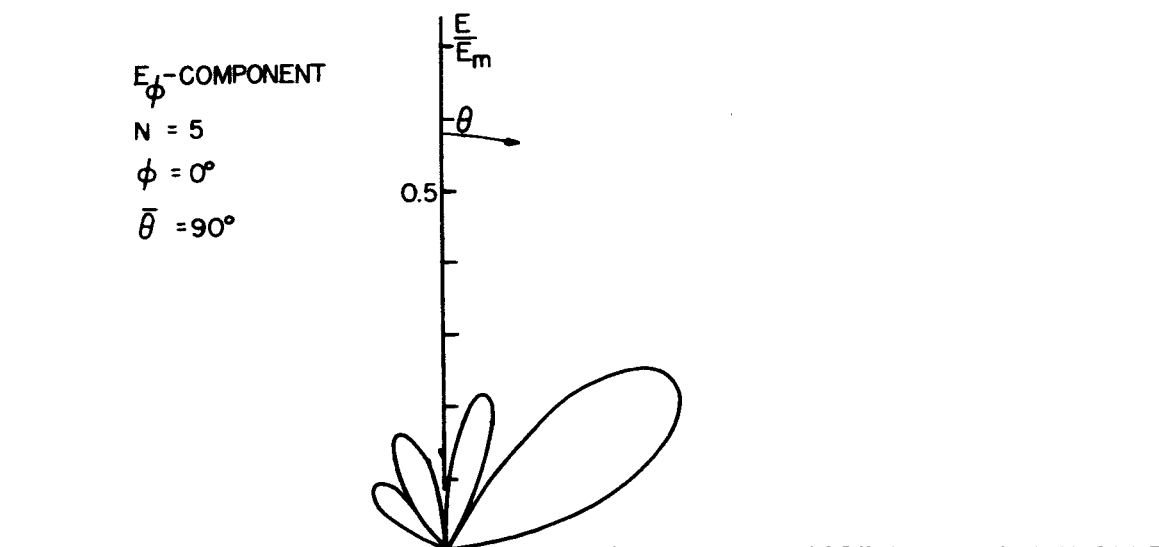
E$_\theta$-COMPONENT

N = 5

ϕ = 0°

$\bar\theta$ = 60°

E$_\phi$-COMPONENT

N = 5

ϕ = 0°

$\bar\theta$ = 60°

FIGURE B-4 THE NORMALIZED FIELD PATTERN OF THE MATRIX ARRAY OF CROSSED SLOT ANTENNAS ILLUSTRATING EFFECT OF BEAM SCANNING

E/Em 1.0

θ

E$_\theta$-COMPONENT

N = 5

ϕ = 0°

$\bar{\theta}$ = 80°

0.5

E/Em

θ

E$_\phi$-COMPONENT

N = 5

ϕ = 0°

$\bar{\theta}$ = 80°

0.5

FIGURE B-5 THE NORMALIZED FIELD PATTERN OF THE MATRIX ARRAY OF CROSSED

SLOT ANTENNAS ILLUSTRATING EFFECT OF BEAM SCANNING

$\frac{E}{E_m}$

1.0

θ

E_θ – COMPONENT

N = 5

$\phi = 0°$

$\bar{\theta} = 90°$

0.5

$\frac{E}{E_m}$

θ

E_ϕ – COMPONENT

N = 5

$\phi = 0°$
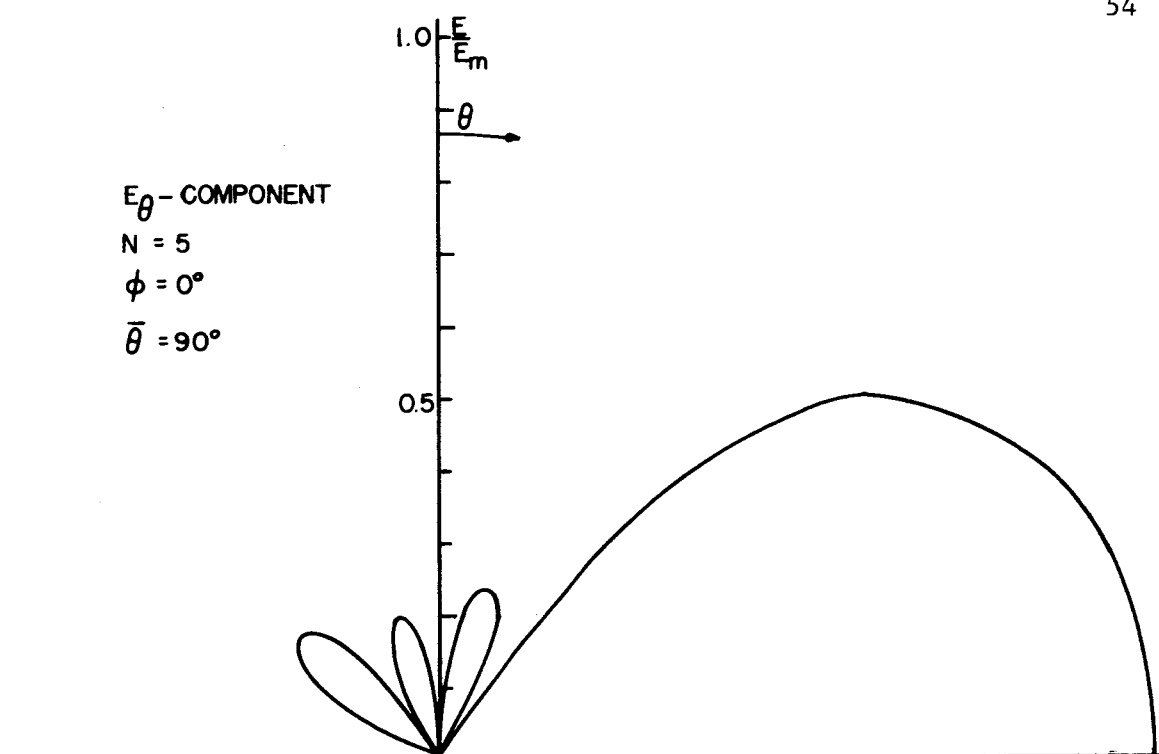
$\bar{\theta} = 90°$

0.5

FIGURE B-6 THE NORMALIZED FIELD PATTERN OF THE MATRIX ARRAY OF CROSSED SLOT ANTENNAS ILLUSTRATING EFFECT OF BEAM SCANNING